



# Performance enhancement of the power penalty in DWDM FSO communication using DPPM and OOK modulation

Ebrahim Eld. Elsayed<sup>1</sup> · Bedir B. Yousif<sup>2</sup> · Mahmoud M. Alzalabani<sup>1</sup>

Received: 16 December 2017 / Accepted: 22 May 2018 / Published online: 26 June 2018  
© Springer Science+Business Media, LLC, part of Springer Nature 2018

## Abstract

This paper presents the design and performance enhancement of the power penalty (PP) in a dense wavelength division multiplexing based on free space optical communication (FSOC) link using digital pulse position modulation (DPPM) and on-off keying (OOK) modulation. Such a system has a high performance, low cost, robust and power efficient, reliable, excessive flexibility, and higher data rate for access networks. The system performance is evaluated for an 8-channel wavelength-division-multiplexing for hybrid fiber FSOC system at 2.5 Gbps on widely accepted modulation schemes under various atmospheric turbulence (AT) regimes conditions. The performance of system is introduced in terms of PP, bit-error rate (BER), transmission distance and the average received optical power. The numerical results shows that the improvement of the PP using DPPM modulation of 0.2–3.0 dB for weak turbulence (WT) regimes for BER of  $10^{-6}$  and above 20, 25 dB for strong turbulence (ST) regimes are reported for BER of  $10^{-6}$  and  $10^{-9}$ , as respectively (depending on the AT level). Further, we develop of improvement the PP caused by multiple-access interference about 6.686 dB which is predicted for target BER of  $10^{-9}$  in WT and 1 dB at target BER of  $10^{-6}$  in ST when the 8 user are active on the system of optical network units. Additionally, the optical power budget and margin losses of a system are calculated with different link length. The proposed approach of DPPM merges superiority with higher enhancement of PP about 0.8 dB for BER equal  $10^{-9}$  at FSO link length  $l_{\text{fso}}=2000$  m compared to OOK at 1 dB for WT. An improvement of 2 dB is observed using the DPPM scheme over an OOK due to capability of detect pulses under background noise conditions with increased receiver sensitivity.

**Keywords** Atmospheric turbulence (AT) · FSO communication (FSOC) · DWDM · Power penalty (PP) · DPPM · Outage probability (OUP) · Amplified spontaneous emission (ASE)

---

**Electronic supplementary material** The online version of this article (<https://doi.org/10.1007/s11082-018-1508-y>) contains supplementary material, which is available to authorized users.

---

✉ Ebrahim Eld. Elsayed  
engebrahem16@gmail.com

Extended author information available on the last page of the article

## 1 Introduction

Although linking communication in free space optical (FSO) spectrum instead of the radio one allows ignoring license requirements, improving security, and transmitting data with a broad spectrum, optical technologies carrier can have access to a good network where they could potentially provide huge bandwidth but it suffers from fluctuations in temperature and pressure that occur in the atmosphere regularly (Chan 2006; Shapiro and Harney 1980). Free-space optical communication (FSOC) includes many improvements as an opportunity to defeat the limitation in capacity of radio frequency (RF), such as easy-to-install, difficult to intercept and license-free. As a result the FSOC performance is even restricted for deep-distance links owing to these obstacles. FSOC using a dense-wavelength-division multiplexing (DWDM) can enhance the number of channels with support from a performance high capacity to reach (32 channel  $\times$  40 Gbps) and are easy to increase a data rate into the FSO for the long-distance data transmission (Ciaramella et al. 2009). FSOC, it is a realistic proposition, which construct a wavelength-division multiplexing (WDM) optical access networks (OAN) in the distribution link since both optical fiber (OF) and FSO systems adopt an identical transmission wavelengths and network components (Ciaramella et al. 2009). There are three types of WDM that are commonly used: coarse WDM (CWDM), dense WDM (DWDM) and broadband WDM. DWDM is a new technology which multiplexes multiples (optical carrier signals) over a singular medium by applying different signals with huge channel capacity and the wavelength range from 1539 to 1565 nm is the most commonly located in conventional band (C-band) and contribute in reducing bandwidth usage and can support capacity to reach Terabits per second and are easily to increase a data rate into the FSO (Ciaramella et al. 2009). The feasibility of WDM FSO networks has been demonstrated experimentally. Passive-optical networks (PON) are the most important competitors for the OAN, where the general network replace the copper on the basis of network access technologies (Karp et al. 1988; Ramaswami and Sivarajan 2002).

DWDM is the next generation of dissemination of hybrid fiber FSOC (HFFSOC) based access network which offers higher bandwidth (Manor and Arnon 2003; Arnon 2003). A common spacing in DWDM is 25, 50, 100, or 200 GHz with channel count leading up to 128 or higher channels at distances of several thousand kilometers from the amplification and regeneration along such a routing. For each optical network unit (ONU), a fixed wavelengths is installed in DWDM-PON and thus a high transfer bandwidth available more full utilize of the in the optical domain (Ansari and Zhang 2013; Zuo and Phillips 2009). DWDM-PON systems offer greater security and increase bandwidth and less loss compared to time division multiplexing/multiple access (TDM/TDMA) (Ciaramella et al. 2009; Aladeloba et al. 2013; Killinger 2002; Monroy and Tangdiongga 2002). Optical amplifier (OA) is important is according to the deep-distances in the free space optics. WDM systems is well reported an Interchannel Crosstalk (ICC) in Ramaswami and Sivarajan (2002). The effects of atmospheric turbulence (AT) accentuated ICC have been investigated in for WDM FSO network (Aladeloba et al. 2013).

When the signal pathways and crosstalk are turbulent independently beyond being physically quite specific so that mutual strength may close tentatively or even considerably exceeds the signal strength in spite of the long-time average signal (LTAS) to crosstalk ratio that resulted a turbulence accentuation of ICC. On-off keying (OOK) and digital pulse position modulation (DPPM) are the most modulation format of AT using intensity of photon. DPPM one concerning the modulation method has supreme power efficiency compared according to OOK (Aladeloba et al. 2012a, b, c; Aldibbiat et al. 2005; Ghassemlooy et al. 2013). It has been successfully implemented in the OF, satellite, terrestrial for FSO and deep space

optical communication. These profits come at the expenditure of higher channel bandwidth demands. DPPM has with success been applied in OF, inter-satellite and deep FSOC and could be a robust competition for terrestrial FSO network (Ghassemlooy et al. 2013; Phillips et al. 1996). Several researches show that DPPM is fitted to FSOC systems wherever dispersion is negligible and it's a lot of power effective schemes compared to OOK (Aladeloba et al. 2012a, b, c; Ghassemlooy et al. 2013). DPPM offer a better error rate performance and a good average received optical power (AROP) requirement efficiency that is critical in obliging with eye safety limitations (Aldibbiat et al. 2005; Ghassemlooy et al. 2013). DPPM satisfies its merits but however at the cost of a bandwidth expansion. Development of the PON idea and a variety of architectures are viable in DWDM. Different wavelengths from several laser light sources in the system raise the problem optical ICC. In DWDM PON, ICC and naturally, unless the wavelength narrow spacing in particular, it will feature a purely amount of contribution to the intensities and no interferometric contribution. Optical amplifiers (OAs) are required for the long haul FSO propagation distances. The optical amplifiers improve the strength of signal on the cost of an amplified spontaneous emission (ASE) noise that limits the system performance (Abtahi et al. 2006).

The reminder paper is structured as follows. Section 2 illustrated the network structure and architecture for DWDM-PON/HFFSOC. Section 3 assessed the AT channel modeling. Section 4 introduces the bit-error rate (BER) analysis. Section 5 presents the BER evaluations for DWDM-PON/HFFSOC systems. The numerical results are presented and discussed in Sect. 6. Section 7 discusses the validations of power penalty compared to the other published papers. Finally, further discussions, conclusions and the future work of research are presented in Sect. 8.

## 2 Network structure and architecture

Figure 1 shows a schematic representation of the planned DWDM-PON based HFFSOC system. The network components encompass a transmitter module which involves of laser for optical signal (OS) generation, a laser driver (LD) and the input data signal and DPPM modulator (DPPM Mod) and receiver modulator with created of a photodetector (PD), filter, and feeder fiber, OA, electrical amplifier (EA), and the comparator circuit (CC) for system decision. Dynamic tracking of a threshold is not needed with DPPM, unlike for some OOK systems. DWDM-PON/HFFSOC relies on multiplexing of the user on incorporating fiber infrastructure employing a specific wavelength for every terminal. This approach creates a virtual link from a point-to-point (POP), which permits full duplex communication with optical bit rates severally of the traffic induced by different users. An erbium doped-fiber amplifier (EDFA) with multi-hop DWDM/relaying are employed for long-distance from the optical line terminator (OLT) to the ONU. Due to the physical of the perfection of demultiplexer (demux) in OLT to move upstream or each Remote Node (RN) for the transfer of downstream an ICC occurs. The effect of AT-emerged ICC in DWDM-PON incorporated with HFFSO a network was investigated in Monroy and Tangdionga (2002). In upstream functional system (UFS) diagram where the ONU transmitter for each transmit OS on wavelengths  $\lambda_1, \lambda_2, \lambda_N$ , where  $N$  is the ONU numbers corresponding toward the diameter  $D_{RX}$  of Receiver Collecting Lenses (RCLs) at the RN and consist of an Optical Band-Pass Filter (OBPF) as shown in Fig. 1a. Each ONU in the UFS has a dedicated independent POP data link to the OLT with a specific fixed optical wavelength as shown in Fig. 1a. In the downstream functional system (DFS) diagram,  $N$  separates transmitter applying to each ONU on a specific wavelength a POP fashion as shown in Fig. 1b. However,

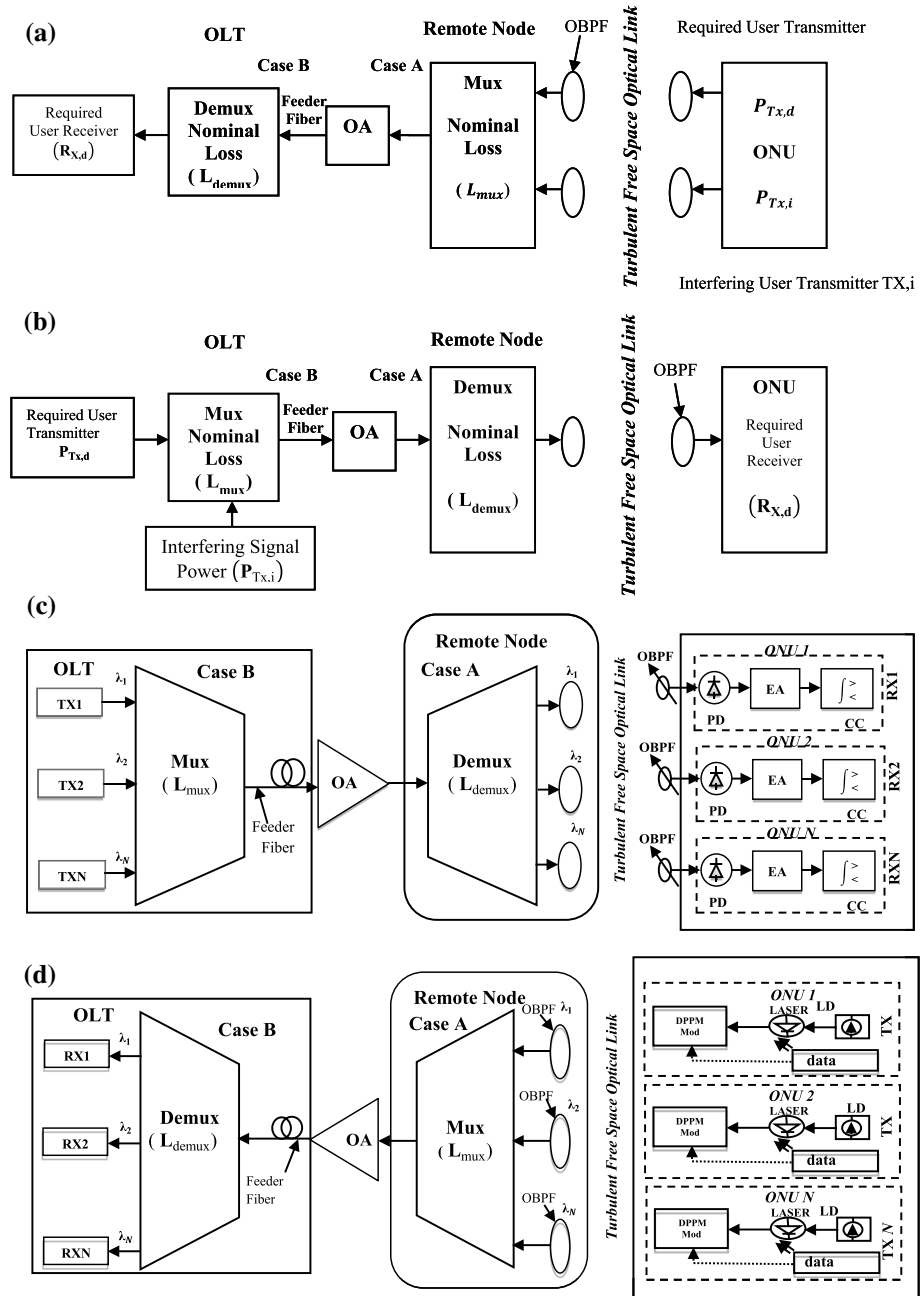


**Fig. 1** A proposed DWDM-PON based hybrid fiber FSOC (HFFSCOC) system for the final distribution stage, with an OA located at the RN (Case A) or at the OLT demux input (Case B). ONUs will be distributed at different angles around the RN **a** Upstream functional system diagram, **b** Downstream functional system diagram, **c** Downstream transmission system (DTS) diagram and **d** Upstream transmission system (UTS) diagram

to reduce fiber nonlinearity, then maximum OLT transmits a power lower than 10 dBm. To restrict background ambient light the downstream collecting lens (CLs) can also include an OBPF as shown in Fig. 1b, while the demux naturally performs the OBPF within the upstream direction. Downstream ICC resulted from the imperfection of the RN demux, but this is not emerged by the AT. Thus, the technique is intensity modulated/direct detection (IM/DD) signal is obtained directly. The downstream transmission system (DTS) diagram RCLs may include an OBPF shown in Fig. 1c to limit background surround light, while the demux inherently precedes the OBPF in the upstream direction. The properties of the CLs used in the tracking and pointing subsystem would vary depending on the FSO link length. In the upstream transmission system diagram (UTS), each ONU has a dedicated specific laser fixed wavelength for a POP optical link to the OLT as illustrated in Fig. 1d. Depending on the FSO link length we choose the suitable lenses in the tracking and pointing subsystem. We use the optimal threshold, frequency spacing and optical wavelengths in OOK modulation of our calculations at the same assumptions for the downstream and upstream transmission. A fiber collimator is used to couples arranged wavelength from each RN RCL through a short length of fiber as in Abtahi et al. (2006) to the Multiplexer (mux). To enhance the signal power through the OF an optical preamplifier of Noise Figure (NF) and Gain (G) can be placed at the RN output. By using an automatic tracking and pointing system, the transmitter divergence angle (TxDA) can be narrowed dimension enough with divergence angle  $\ll 1$  mrad to achieve the alignment with adjusting the focal lengths and position of the lenses, which allows a collect larger proportion of transmitted power and secure transmission.

### 3 Atmospheric turbulence channel modeling

Atmospheric scintillation takes place due to the heat difference between the earth’s surface and pressure caused refractive index variations of the atmosphere along the data link channel, leading to speedy change of the received signal, divergence in degree of continuity of the OS and too insufficient BER. These implements of conflict, weak, moderate, and strong are described utilizing the Probability Density Function (pdf) of Gamma–Gamma (GG) and given as (Andrews et al. 2001; Andrews and Phillips 2005; Majumdar 2005; Khalighi et al. 2009; Al-Habash et al. 2001)

$$p_{GG}(h_z) = \frac{2(\alpha\beta)^{(\alpha+\beta)/2}}{\Gamma(\alpha)\Gamma(\beta)} h_z^{((\alpha+\beta)/2)-1} K_{\alpha-\beta}\left(2\sqrt{\alpha\beta}h_z\right); \quad h_z > 0, \tag{1}$$

where  $h_z = h_d$  or  $h_i$  is the attenuation owing to AT for the required signal ( $h_{sig}$ ) or interfere ( $h_{int}$ ),  $\alpha$  and  $\beta$  are the effective quantity of large and small scale eddies due to the scattering process respectively,  $K_n(\cdot)$  is a modified Bessel Function (MBF) (second kind, order  $n$ ), and  $\Gamma(\cdot)$  is the Gamma function. The signal and interferer (SAI) travels independently over physically separate pathways in the UTS and then have uncorrelated disturbance; hence, their GG pdfs are each dealt with independently. The parameter  $\alpha$  and  $\beta$  are given as (Andrews et al. 2001; Andrews and Phillips 2005; Majumdar 2005; Khalighi et al. 2009; Al-Habash et al. 2001)

$$\alpha = \left\{ \exp \left[ \frac{0.49\sigma_R^2}{\left(1 + 0.65 d^2 + 1.11\sigma_R^{12/5}\right)^{7/6}} \right] - 1 \right\}^{-1}, \tag{2}$$

$$\beta = \left\{ \exp \left[ \frac{0.51\sigma_R^2 \left( 1 + 0.69\sigma_R^{12/5} \right)^{-5/6}}{1 + 0.9d^2 + 0.62d^2\sigma_R^{12/5}} \right] - 1 \right\}^{-1}, \tag{3}$$

$$d = \sqrt{kD_{RX}^2/4l_{fso}} \tag{4}$$

where  $d$  is the normalized RCLS,  $C_n^2$  is the refractive index structure (RINS) parameter (ranging from  $\approx 1 \times 10^{-17} \text{ m}^{-2/3}$  to  $\approx 1 \times 10^{-13} \text{ m}^{-2/3}$ ),  $l_{fso}$  is the FSO channel length,  $k = 2\pi/\lambda$  is the wave number and  $\lambda$  is the wavelength are given as Andrews and Phillips (2005), Majumdar (2005), Khalighi et al. (2009) and Al-Habash et al. (2001). Table 1 presents the turbulence conditions regimes for FSO link length ( $l_{fso}$ ) = 1000 m come from  $C_n^2$ . The Rytov variance (RVAR) distinguishes the various link turbulence regimes  $\sigma_R^2$ , if the resulting  $\sigma_R^2 < 1$ , we have weak turbulence (WT); if  $\sigma_R^2 \approx 1$ , we have Moderate Turbulence (MT) and if  $\sigma_R^2 > 1$ ; we have strong turbulence (ST), and if saturated turbulence  $\sigma_R^2 \rightarrow \infty$  are given as from (Andrews and Phillips 2005; Khalighi et al. 2009)

$$\sigma_R^2 = 1.23 C_n^2 k^{7/6} l_{fso}^{11/6} \tag{5}$$

### 4 Bit error rate (BER) analysis

The BERs conditional under the hypothesis of separate signal and ICC for UTS and DTS, the average turbulence which accentuated ICC BER of given specific transmitter powers for the OS and ICC (Aladeloba et al. 2013)

$$\overline{BER} = \int_0^\infty \int_0^\infty BER(h_{sig}, h_{int}) p_{GG,sig}(h_{sig}) p_{GG,int}(h_{int}) dh_{sig} dh_{int}, \tag{6}$$

where  $p_{GG,sig}(h_{sig})$  and  $p_{GG,int}(h_{int})$  are respectively, the SAI GG-pdfs each with various value  $\alpha$ ,  $\beta$  and  $\sigma_R^2$  as written in Manor and Arnon (2003), Phillips et al. (1996), Abtahi et al. (2006) and Andrews et al. (2001). Using Gaussian beam approximation (GBA) methods, the BER dependent on ( $h_{sig}$ ) and ( $h_{int}$ ) for UTS with single ICC (Aladeloba et al. 2013)

$$BER(h_{sig}, h_{int}) = \frac{1}{4} \operatorname{erfc} \left( \frac{Q(h_{sig}, h_{int})}{\sqrt{2}} \right) \tag{7}$$

**Table 1** The turbulence conditions regimes for FSO link length with ( $l_{fso}$ ) = 1000 m of  $C_n^2$

Turbulence regimes	$C_n^2$
Weak turbulence (WT)	$1 \times 10^{-17} \text{ m}^{-2/3}$
Moderate turbulence (MT)	$8.4 \times 10^{-15} \text{ m}^{-2/3}$
Strong turbulence (ST)	$1 \times 10^{-13} \text{ m}^{-2/3}$

$$Q(h_{sig}, h_{int}) = \frac{i_{1,0}(h_{sig}, h_{int}) - i_{0,1}(h_{sig}, h_{int})}{\sigma_{1,0}(h_{sig}, h_{int}) + \sigma_{0,1}(h_{sig}, h_{int})} \tag{8}$$

$$i_{d_{sig}, d_{int}}(h_{sig}, h_{int}) = i_{d_{sig}}(h_{sig}) + i_{d_{int}}(h_{int}) \tag{9}$$

where  $i_{d_{sig}, d_{int}}(h_{sig}, h_{int})$  is the outputs for signal ( $d_{sig} =$  zero or one) and interferer ( $d_{int} =$  zero or one) of decision circuit (DC). where  $i_{d_{sig}, d_{int}}(h_{sig}, h_{int})$  is the resulting signal  $i_{d_{sig}}(h_{sig}) + i_{d_{int}}(h_{int}) = (d_{sig} =$  zero or one) and interferer ( $d_{int} =$  zero or one) current at the DC are written as (Aladeloba et al. 2013),  $i_{d_{sig}}(h_{sig}) = \alpha d_{sig} RP_{R, sig}(h_{sig})$  and  $i_{d_{int}}(h_{int}) = \alpha d_{int} RP_{R, int}(h_{int})$  is SAI current for data one and zero, are, respectively.  $P_{R, sig}$  and  $P_{R, int}$  are the instantaneous and interferer AROP, respectively.  $r$  is the extinction ratio and  $R = \eta q/E$  is the responsivity (in A/W),  $\eta$  is the PD quantum efficiency,  $q$  is the electron charge,  $E = h\nu$  is the photon energy,  $h$  is Planck's constant and  $\nu$  is the optical frequency. The total OLT Thermal Receiver Noise Variance (TRNVAR)  $\sigma_{d_{sig}, d_{int}}^2$  is the summation of the shot noise signal, amplified spontaneous emission (ASE) shot noise, signal-ASE Beat Noise (ASEBN), and ASE-ASE beat noise variance, given respectively in Eqs. (10–13). An integrate-and-dump receiver is assumed at the DC with electrical bandwidth  $B_e = 1/2 T_b$ ,  $T_b = 1/ R_b$  and  $R_b$  is the data rate,  $B_e = R_b/2$ ,  $m_t$  is ASE noise polarization states and ASE Noise (ASEN) Power Spectral Density (PSD) in a single ploarization state.  $B_0$  is the optical bandwidth:

$$\sigma_{shot-d_{sig}, d_{int}}^2 = 2qi_{d_{sig}, d_{int}}(h_{sig}, h_{int})B_e, \tag{10}$$

$$\sigma_{shot, ASE}^2 = 2m_t B_0 N_o qR B_e, \tag{11}$$

$$\sigma_{sig-d_{sig}, d_{int}-ASE}^2 = 4RN_o i_{d_{sig}, d_{int}}(h_{sig}, h_{int})B_e, \tag{12}$$

$$\sigma_{ASE-ASE}^2 = 2m_t R^2 N_o^2 B_0 B_e. \tag{13}$$

### 4.1 Upstream transmission system

For the overall performance evaluations, it is assumed to have signal multiplexer/demultiplexer losses  $L_{mux}$  and  $L_{demux} (\leq 3.5$  dB) (Monroy and Tangdiongga 2002), a contiguous-channel additive loss  $L_{mux, contiguous}$  (typically > 30 dB), and non-a contiguous-channel additive loss  $L_{mux, non-contiguous}$  (generally > 35 dB). Equations (6–13), can be employed for the system of specific computations. The Single Crosstalk (SC) channel is relevant a predominant interferer occurs (e.g., in some slightly DWDM network). There is also the probability of systems where some transportation channel is FSOC and OF. At PDs of the OLT photodiodes for the required SAI is given for the AROP, respectively, by equation written in (Aladeloba et al. 2013)

$$P_d(h_d) = GP_{u, d} h_d L_{fso, d} L_{bs, d} \eta_{c, d} L_{mux} L_{fiber} L_{demux}, \tag{14}$$

$$P_i(h_i) = GP_{u_{T,i}} h_i L_{fso,i} L_{bs,i} \eta_{c,i} L_{mux} L_{fiber} L_{demux} L_{demux,XT}, \tag{15}$$

where  $G$  is gain optical amplifier,  $L_{demux,XT}$  is the crosstalk (XT) i.e. additional losses (above  $L_{demux}$ ) the interferer has when connected onto the OS photodiode by the demultiplexer.  $P_{u_{T,d}}$  and  $P_{u_{T,i}}$  are the signal and interferer of ONU transmitting powers, respectively

$$L_{fso} = 10^{(-\alpha_{fso} l_{fso}/10)} \tag{16}$$

$$L_{fiber} = 10^{(-\alpha_{fiber} l_{fiber}/10)} \tag{17}$$

where  $L_{fso}$  and  $L_{fiber}$  (OFL) are the FSO and OF Losses where  $\alpha_{fiber}$  and  $\alpha_{fso}$  are the attenuation coefficients of OF and FSO, respectively, (in dB/km).  $l_{fiber}$  is the channel length for OF in (km). The nominal demux loss  $L_{demux}$ /multiplexer (mux) loss  $L_{mux}$  is about 3.5 dB (Monroy and Tangdiongga 2002), while the interferer’s demux loss  $L_{demux,XT}$  is the other loss that interferer experiences upon connecting to the required signal wavelength port, and also defines the signal-to-crosstalk ratio ( $C_{XT}$ ) (in the case when the input signal power (SIGP) and crosstalk power (CXTP) are corresponding. Under weather conditions, signal attenuation is higher intense and the FSOC length is limited. The beam spreading loss  $L_{bs}$  in the FSOC link for the desired SAI can be calculated from (Andrews and Phillips 2005; Majumdar 2005)

$$L_{bs} = \left( \frac{D_{RX}}{\theta l_{fso}} \right)^2 \tag{18}$$

and  $\eta_c$  is the coupling loss for both the SAI is determined from Dikmelik and Davidson (2005). In the UTS Case A, the obtained ASEN PSD in the single polarization state at the photodiode can be written as  $N_{o,OA} = 0.5(NFG - 1) h \nu L_{fiber} L_{demux}$  where  $G$  and  $NF$  are the OA gain and noise figure, respectively. Various qualities of  $N_o$  rise depending on the OA stand, while in Case B, the collected ASEN PSD as can be written as  $N_o = N_{o,OA} L_{demux,XT}$ .

### 4.2 Downstream transmission system

The downstream ICC is not emphasized disturbance, as rejecting wavelength change shape on  $\sigma_R^2$  it passes through the same atmospheric direction as the signal. In the DTS Case A, the received ASEN in the original emission state at the PD is expressed as  $N_{o,OA} = 0.5(NFG - 1) h \nu L_{demux} L_{fso} L_{bs}$ , but in Case B, the obtained ASEN PSD, it is given as  $N_o = N_{o,OA} L_{demux,XT}$  (Aladeloba et al. 2013). The AROP at the ONU photodiodes for required SAI is presented, respectively, as written in (Aladeloba et al. 2013; Mbah et al. 2016)

$$P_{d_{R,sig}}(h_Z) = GP_{d_{T,d}} h_Z L_{fso} L_{bs} L_{mux} L_{fiber} L_{demux} \tag{19}$$

$$P_{i_{R,int}}(h_Z) = GP_{d_{T,i}} h_Z L_{fso} L_{bs} L_{mux} L_{fiber} L_{demux} L_{demux,XT} \tag{20}$$

where  $P_{d_{T,d}}$  and  $P_{d_{T,i}}$  are the respective downstream OLT transmitter power of SAI.



## 5 BER evaluations for hybrid DWDM PON FSOC systems

This section includes evaluations the BER for hybrid DWDM-PON/FSOC in DPPM and OOK modulation. DWDM-FSO technology is a key component of next generation needs designed and simulated to serve as Long Reach Passive Optical Network (LR-PON) for achieving higher rate, immense capability, and allows operators to deliver high information measure to multiple using one wavelength of upstream transmission and another wavelength for upstream transmission. DWDM PON is linked a multi-wavelengths optical line terminator to optical network units over an interconnecting OF system. The optical line terminator is one of the foremost necessary of the network. It provides an interface between core network and PON network. OA positioning with two other sources of amplifier location is Case A at RN and at the OLT Case B. In the UST Case A, the ASEN expertise loss owing to feeder OF attenuation and OLT demux loss, while in the UST Case B, the ASEN suffers from OLT demux losses in OLT only. In some Cases the position of the UST OA may also no longer do enough distinction to the overall performance, considering that the optical signal-to-noise ratio (OSNR) range by way of only approximately 4 dB among Case A and Case B (for 20 km OF). In the DTS Case A, the ASEN suffers RN demux losses, AT power loss, and beam divergence spreading loss, while in the DTS Case B, the ASEN moreover experiences OF attenuation feeder fiber. ONU is access services. For both DTS and UTS areas directions, the OLT connected with ONUs via  $N$  intermediate relays ( $R_i, i=1, 2 \dots N$ ), together with RN. Table 2 is a key parameter used in the calculations (Aladeloba et al. 2013; Mbah et al. 2016) and [present]. Forward error correction (FEC) is able to much better performance. Note, however, that the proper relation between the LTAS BER before and after the forward error corrections would take the FEC to enter the analysis, e.g., within Eq. (6). Dispersion and nonlinear effectiveness at OF are rejected for

**Table 2** Key parameters used in the calculations

Parameters	Description	Values in Aladeloba et al. (2013)	Values in Mbah et al. (2016)	Present work
$R_b$	Binary data rate	2.5 Gbps	2.5 Gbps	2.5 Gbps
$B_o$	Demux or OBPF channel bandwidth	60 GHz	76 GHz	60 GHz
$\lambda$	Desired signal wavelength	1550 nm	1550 nm	1550 nm
$\theta_{XT}$	Transmission divergence angle	0.2 mrad	0.2 mrad	0.2 mrad
$D_{RX}$	Receiver Cls diameter	13 mm	13 mm	17 mm [Present]
$r$	Extinction ratio	10 dB	10 dB	10 dB
$\eta$	Quantum efficiency	0.8	0.8	1 [Present]
NF	Amplifier noise figure	4.77 dB	4.77 dB	4.77 dB
$L_{iso}$	Maximum FSO link length	2 km	2 km	4 km [Present]
$L_{fiber}$	Feeder fiber length	20 km	20 km	20 km
$\alpha_{fiber}$	Feeder fiber attenuation	0.2 dB/km	0.2 dB/km	0.2 dB/km
$\alpha_{fso}$	Atmospheric channel attenuation [clear air]	0.2 dB/km	0.2 dB/km	0.2 dB/km
$m_t$	ASE noise polarization states	2	2	2
G	Optical preamplifier gain	30 dB	30 dB	30 dB
$L_{demux}$	Signal mux/demux loss	3.5 dB	3.5 dB	3.5 dB

a 20 km feeder, only particularly minor Power Penalties (PP). The RCL diameter option (13 mm) well reported in Aladeloba et al. (2013), Mbah et al. (2016) and Vetelino et al. (2007) but we assume the RCL diameter (17 mm) is coherent with this work and signal mux/demux loss  $L_{demux}$  (3.5 dB) (Monroy and Tangdionga 2002; Lee et al. 2006). OOK modulation in DWDM FSOC is the oftenest performance generally used IM/DD. This approach provides an easy implementation and minimum cost (Badar and Jha 2017). Seeks to beat the irreducible Error Floors (EFs) of OOK have directed on the study of adaptive detection threshold (ADT). For calculating the require average received power, there is no single equation at a fixed BER by maintaining the BER at a fixed value and restructure the code for finding the BER to be able to calculate the average power that can give the fixed BER. This can be done using the root finding technique. Basically to find an average power value that will result in a BER value above the fixed BER value and another average power value that will result in a BER value below the fixed BER value. Then use the average power that gave the higher and lower BER values as the upper and lower limit of the root finding search and then keep dissecting the space in between those two limits until get the approximate average power that can give the fixed BER.

### 5.1 DPPM crosstalk modeling

The DPPM format is achieving a significant improvement in power efficiency. The DPPM modulation offers greater channel bandwidth requirements. DWDM DPPM format, is simple case of a single contiguous interferer However, the evaluations accentuated ICC, where, M bits is the frame assigned with the raw DR  $R_b$ , are assigned to a frame, where each block of  $b$  bits is mapped to one of M feasible symbols ( $s_0, s_1, s_M$ ) where  $n = 2^M$  equal-sized time slots  $t_s = M/nR_b$ , where  $T_b = 1/R_b$ , where M is referred to as the Coding Level (COL). For illustration, at the binary DR of 2.5 Gbps, DPPM Frames (DPPMF) for  $M=2$  include four slots,  $t_s = 2 T_b /4$ ,  $t_s = 2/4 \times 2.5 \text{ GHz} = 1/5 \text{ GHz}$ , each and therefore the pulse in each DPPMF shows a 2-bit word transferred at a slot rate of 5 GHz. For  $M=4$  contain = 16 slots shows example of time-waveforms of an OOK Non-Return-to-Zero (NRZ) and the equivalent 16-DPPM signal ( $M=4$ ) (Mbah et al. 2014). Systems bandwidth increases with rising COL and proper spacing is needed between the wavelengths for operations with significant COL, OSs encompass not alone data signal but also background noises and SAI with the AROP of background power  $P_b$  and power transmitter  $P_t$  int. The Means and Variances (MEAVAR) of the random variables, both are describing the conjunction over the slot that consists of particularly the Signal Pulse (SP), especially Crosstalk Pulse (CP), both SP and CP pulses and no pulses (i.e. empty slot) are determined and, respectively, the general equations for the UTS are derived in (21–25), the equations for the DTS are regain by changing the losses due to AT for the required SAI ( $h_d, h_i$ ) with  $h_z$  written as (Aladeloba et al. 2012a, b, c; Mbah et al. 2014).

$$\mu_{X_{sig,int}}(h_d, h_i) = \frac{LRqN_o}{t_s} + Gq(sigRP_d(h_d) + intR_iP_i(h_i)) \tag{21}$$

$$\sigma_{X_{sig,int}}^2(h_d, h_i) = \sigma_{ih}^2 + \left( \frac{(LRq^2N_o(1 + LRq^2N_o))}{t_s^2} \right) + Gq^2 \left[ \begin{array}{l} (R + 2R^2N_o) \frac{sigP_d(h_d)}{t_s} \\ + (R_i + 2R_i^2N_{o,i}) \frac{intP_i(h_i)}{t_s} \end{array} \right] \tag{22}$$

where sig/int = 0 or 1 relying on the existence of SP/CP pulse in slot.  $\sigma_{th}^2$  is TRNVAR of DPPM,  $L = B_o m_t t_s$  is the product of temporal and spatial modes (Aladeloba et al. 2012a, b, c),  $B_o$  is the demultiplexer or OBPF channel bandwidth, and  $m_t$  is the number of ASEN polarization states. The ASEN for PSD in a specific polarization state at the photodiode is  $N_o$ . MEAVAR have been obtained with modifications to account for crosstalk–ASEBN affecting the interferer and the needed signal experiences the same ASEN at the OA output (Aladeloba et al. 2012a, b, c)

$$P_{we(l,r)}(h_d, h_i) \geq \prod_{\substack{j=1 \\ j \neq sig\ slot}}^n P(X_{1,int} > X_j | h_d, h_i) \tag{23}$$

where  $X_j$  is the non-signal slot  $X_{0,int}$  contents (Mbah et al. 2014)

$$P_{we(l,r)}(h_d, h_i) \leq 1 - (1 - P(X_{0,0} > X_{1,int} | h_d, h_i))^{n-1-(l-r)} 1 - P(X_{0,1} > X_{1,int} | h_d, h_i)^{l-r} \tag{24}$$

Assuming that the random variables  $X_{1,int}$  and  $X_{0,int}$  are Gaussian, the expression  $P(X_{0,int} > X_{1,int} | h_d, h_i)$  using GBA is of the general form (Mbah et al. 2014)

$$P(X_{0,int} > X_{1,int} | h_d, h_i) = 0.5 \operatorname{erfc} \left( \frac{\mu_{X_{1,int}}(h_d, h_i) - \mu_{X_{0,int}}(h_d, h_i)}{\sqrt{2(\sigma_{X_{1,int}}^2(h_d, h_i) + \sigma_{X_{0,int}}^2(h_d, h_i))}} \right) \tag{25}$$

The BERs conditional for the UTS and DTS on the turbulence and crosstalk frame overlap, respectively are given as

$$BER_{U_l}(h_d, h_i, n_1) = p_{f(l)}(n_1) \frac{n}{2(n-1)} \times (p_{s(l)}(1)P_{we(l,1)}(h_d, h_i) + p_{s(l)}(0)P_{we(l,0)}(h_d, h_i)) \tag{26}$$

$$BER_{D_l}(h_z, n_1) = p_{f(l)}(n_1) \frac{n}{2(n-1)} \times (p_{s(l)}(1)P_{we(l,1)}(h_z) + p_{s(l)}(0)P_{we(l,0)}(h_z)) \tag{27}$$

where  $p_{f(l)}(n_1)$  is the probability of  $l$  CP shooting the Single Frame (SF). Also  $p_{s(l)}(r)$  is the probability of  $r$  out of  $l$  CP shooting the single slot are calculated the same as in Mbah et al. (2014).  $P_{we(l,1)}(h_d, h_i)$  and  $P_{we(l,0)}(h_d, h_i)$  are calculated using Eq. (24) for  $r = 1$  and 0 which represent probability error for interfere and the desired signal for different turbulent regimes in the UTS. Also  $P_{we(l,1)}(h_z)$  and  $P_{we(l,0)}(h_z)$  are computed using Eq. (24) where SAI for the same AT channel link in the DTS. The total BER in the existence of the turbulence and crosstalk for UTS and DTS determined using Eqs. (26), (27) respectively

$$\overline{BER}_U = \int_0^\infty \int_0^\infty \frac{1}{n} \sum_{n_1=0}^{n-1} \sum_{l=0}^2 BER_{U_l}(h_d, h_i, n_1) p_{GG,d}(h_d) p_{GG,i}(h_i) dh_d dh_i \tag{28}$$

$$\overline{BER}_D = \int_0^\infty \frac{1}{n} \sum_{n_1=0}^{n-1} \sum_{l=0}^2 BER_{D_l}(h_z, n_1) p_{GG,d}(h_z) dh_z \tag{29}$$

The SF and crosstalk with fixed mis-alignment, (28) and (29) are modified to eliminate conditions of averaging over all values for the UTS and DTS of  $(n_1)$ .

**5.2 Error floors analysis in the case of adaptive and fixed detection thresholds**

This section includes the analytical mathematical model of the EFs that rely on OOK with adaptive and fixed detection threshold modulation for a general depiction of functional DWDM-FSO links. The result obtained proved a further improvement with the modified OOK is used to eliminate the EFs that occurs in the case of the (Signal with AT, Interferer with No AT (TurbuSi,XT)). The resulting of analysis the EF are outlined in Table 3, where  $K_{\alpha-\beta}(\cdot)$  denotes the MBF of the second kind with order  $\alpha-\beta$  (Yang et al. 2016).

**5.2.1 Mathematical model derivation of OOK with adaptive detection threshold**

$$BER (P_{R, sig}(1)) = \frac{1}{4} \operatorname{erfc} \left( \frac{2(r-1) R P_{R, sig}(1) / (r+1)}{2 q B_e R P_{R, sig}(1) + \sigma_{th}^2} \right) \tag{30}$$

In the second one, it has the form

$$BER = \frac{1}{4} \int_0^\infty \operatorname{erfc} \left( \frac{2(r-1) R \cdot P / (r+1)}{2 q B_e R \cdot P + \sigma_{th}^2} \right) p_{GG} \left( \frac{P}{P_{R, sig}(1)} \right) dP \tag{31}$$

where

$$p_{GG} \left( \frac{P}{P_{R, sig}(1)} \right) = \frac{2(\alpha\beta)^{(\alpha+\beta)/2}}{\Gamma(\alpha)\Gamma(\beta)} \left( \frac{P}{P_{R, sig}(1)} \right)^{((\alpha+\beta)/2)-1} K_{\alpha-\beta} \left( 2\sqrt{\alpha\beta \frac{P}{P_{R, sig}(1)}} \right) \tag{32}$$

Finally, in the last case the dependence is the following:

$$BER = \frac{1}{4} \int_0^\infty \operatorname{erfc} \left( \frac{2(r-1) R \cdot P (1 - 1 / C_{XT}) / (r+1)}{2 q B_e R \cdot P (1 + 1 / C_{XT}) + \sigma_{th}^2} \right) p_{GG} \left( \frac{P}{P_{R, sig}(1)} \right) dP \tag{33}$$

Here, the major challenge consists in taking integrals in the right hand sides of the Eqs. (31) and (33) properly. To find correct values for the integral limits in these equations, one should examine the dependence that is the following as written in (Andrews and Phillips 2005; Mbah et al. 2016; Al-Habash et al. 2001)

$$p_{GG}(h_z) = \frac{2(\alpha\beta)^{(\alpha+\beta)/2}}{\Gamma(\alpha)\Gamma(\beta)} h_z^{((\alpha+\beta)/2)-1} K_{\alpha-\beta} \left( 2\sqrt{\alpha\beta h_z} \right); \quad h_z > 0, \tag{34}$$

where  $h_z$  is the attenuation owing to AT.

Since

$$\int_{10^{-12}}^3 p_{GG}(h_z) dh_z = 0.9725 \tag{35}$$

**Table 3** pdf and error floor terms for different atmospheric turbulence channel models. (Reproduced with permission from Yang et al. 2016)

Turbulence models	pdf	Error floors
Lognormal	$\frac{1}{\sqrt{2\pi\sigma I}} \times \exp\left\{-\frac{(hI+\sigma^2)^2}{2\sigma^2}\right\}$	$(1 - p_1)Q\left(\frac{hI_{th} - \ln\xi + \sigma^2/2}{\sigma}\right) + p_1Q\left(\frac{\ln(\zeta+\xi) - \ln I_{th} - \sigma^2/2}{\sigma}\right)$
K-Distribution	$\frac{2\alpha^{-1}}{\Gamma(\alpha)} I^{\frac{\alpha-1}{2}} \times K_{\alpha-1}\left(2\sqrt{\alpha I}\right)$	$(1 - p_1)\left\{1 - \frac{1}{2}\right\} \left[ h(1, \alpha, T_{th}, \xi) + h(\alpha, 1, T_{th}, \xi) \right] + p_1 \left\{ \frac{1}{2} \left[ h(1, \alpha, T_{th}, 2+\xi) + h(\alpha, 1, T_{th}, 2+\xi) \right] \right\}$
Gamma-Gamma	$\frac{2(\alpha\beta)^{\frac{\alpha+\beta}{2}}}{\Gamma(\alpha)\Gamma(\beta)} I^{\frac{\alpha+\beta}{2}-1} \times K_{\alpha-\beta}\left(2\sqrt{\alpha\beta I}\right)$	$(1 - p_1)\left\{1 - \frac{1}{2}\right\} \left[ h(\beta, \alpha, T_{th}, \xi) + h(\alpha, \beta, T_{th}, \xi) \right] + p_1 \left\{ \frac{1}{2} \left[ h(\beta, \alpha, T_{th}, 2+\xi) + h(\alpha, \beta, T_{th}, 2+\xi) \right] \right\}$
Negative exponential	$\frac{1}{\mu} \exp\left\{-\frac{I}{\mu}\right\}$	$(1 - p_1) \exp\left(\frac{T_{th}}{\mu\xi}\right) + p_1 \left\{ 1 - \exp\left[\frac{T_{th}}{(2+\xi)\mu}\right] \right\}$

With performing the integration in Eqs. (31) and (33) from  $10^{-12} \cdot P_{R,sig}(1)$  to  $3 \cdot P_{R,sig}(1)$  one can count on the accuracy that does not exceed a few percent. For instance, one can try  $10^{-12}$  for the lower limit and  $10^{-3}$  for the upper one. However, the arbitrary choice of limits can lead to the normalization of GG pdf that does not equal to 1 exactly. Therefore, one can introduce the normalization constant  $A$  in this function

$$P_{GG}\left(\frac{P}{P_{R,sig}(1)}\right) = \frac{2(\alpha\beta)^{\frac{(\alpha+\beta)}{2}}}{\Gamma(\alpha)\Gamma(\beta)}A\left(\frac{P}{P_{R,sig}(1)}\right)^{((\alpha+\beta)/2)-1} \times K_{\alpha-\beta}\left(2\sqrt{\alpha\beta\frac{P}{P_{R,sig}(1)}}\right) \quad (36)$$

### 5.2.2 OOK with fixed detection threshold

The received signal ( $r = \xi I + N$ ) in the low state, where  $N$  (noise PSD) and  $I_s = \xi I$  optical received independent and  $\xi$  is low and high offset that result from use with  $r$  (Yang et al. 2016), since  $I_s, N$  are assumed to be independent.

$$f(r|s_0) = \frac{1}{\xi}f_I\left(\frac{r}{\xi}\right) * f_N(r) = \int_0^\infty \frac{1}{\sqrt{2\pi}\sigma_x} \exp\left(-\frac{\left(\ln\frac{x}{\xi} + \frac{\sigma^2}{2}\right)^2}{2\sigma^2}\right) \times \frac{1}{\sqrt{2\pi}\sigma_y} \exp\left(-\frac{(r-x)^2}{2\sigma_y^2}\right) dx \quad (37)$$

where  $*$  symbolize for the convolution process, and  $f_N(r) = \frac{1}{\sqrt{2\pi}\sigma_y} \exp\left(-\frac{(r)^2}{2\sigma_y^2}\right)$  denotes the noise pdf. For a given fixed detection threshold (FDT)  $T_{th}$ , the false alarm probability  $P_F$  and the miss probability  $P_M$  can be respectively is given by (Yang et al. 2016)

$$P_F = \int_{T_{th}}^\infty f(r|s_0) dr = \int_{T_{th}}^\infty \left(\frac{1}{\xi}\right) f_I\left(\frac{r}{\xi}\right) * f_N(r) dr \quad (38)$$

$$P_M = \int_{-\infty}^{T_{th}} f(r|s_1) dr = \int_0^{T_{th}} \left(\frac{1}{2+\xi}\right) f_I\left(\frac{r}{2+\xi}\right) * f_N(r) dr. \quad (39)$$

Assuming that  $p_1$  shows a priori probability that “1” is sent, i.e.,  $p_1 = 1/2$  means “0”s and “1”s are equally likely to be sent, one can write that the BER for OOK using FDT  $T_{th}$  as

$$P_e = (1 - p_1)P_F + p_1P_M \quad (40)$$

where  $T_{th}$  is FDT,  $P_F$  and  $P_M, Q_{(x)} = \frac{1}{\sqrt{2\pi}} \int_x^\infty e^{-\frac{t^2}{2}} dt$  is the Gaussian Q-function in fixed and unoptimized detection threshold.

### 5.3 Mathematical model of power penalty

This section is mainly dealt with the deterioration led to by the optical crosstalk, PP can be referred to as the devaluation othe difference of Optical Power (OP) level between the “1” and the “0” states and this is expressed in the following equation (Gyselings et al. 1999)

$$\epsilon_x = \left\{ \frac{P((t_1)|d_s(t_1) = 1) - P((t_0)|d_s(t_0) = 0)}{A^2/2} \right\} \tag{41}$$

where  $P((t_1)|d_s(t_1) = 1)$  is the OP in case “1” and the  $P((t_0)|d_s(t_0) = 0)$  is the OP in case “zero”. The PP will be:

$$P_x = -10. \log \{ \epsilon_x \} \tag{42}$$

In general terms, the spectral emission from a typical LD agrees fairly well to a Gaussian distribution, which then provides a direct analytic explanation for operation in any model. Corresponding to Gaussian placement in the analytical model, the MEAVAR for a random variable will be:

$$E[\epsilon_X] = 1 \tag{43}$$

$$\text{var}[\epsilon_X] = \sum_i^N \delta_i \tag{44}$$

Since  $E[\epsilon_X]$  and  $\text{var}[\epsilon_X]$  calculate the mean and variance of a random variable, respectively. With GA distribution, considered the following:

$$\text{BER} = P \left[ \epsilon_X \leq \left( 1 - 6 \sqrt{\sum_{i=1}^N \delta_i} \right) \right] = 10^{-9} \tag{45}$$

Here the purpose of as a model of benefit for determining the certainty for the penalty analysis. But this is not automatically an assurance need for actual system design, as this model does not actually have to correspond with the generally employed BER amount of value at  $10^{-9}$ . However, with this level of assurance for calculating crosstalk (XT) penalty:

$$P_x == -10. \log \left( 1 - 6 \sqrt{\sum_{i=1}^N \delta_i} \right) \tag{46}$$

where  $P_x$  represents the PP of AROP signal, (N) is the number of XT elements and  $\delta_i$  is the XT coupling coefficient. Equation (46) shows the PP to the obtained OS in the process where the optical receiver noise is controlled by thermal noise. But for further exact evaluation if the detection is signal spontaneous beat noise dominated (47) the equation will be

$$P_x == -5. \log \left( 1 - 6 \sqrt{\sum_{i=1}^N \delta_i} \right) \tag{47}$$

The Eqs. (46) and (47) have been employed for investigating the implementation proceeds as designs for PP of the DWDM FSOC.

### 5.4 Optical power budget analysis

The mean to OAN distance is optical power budget (OPB) the amount of light possible to produce at OF link. OFL or overall attenuation is the amount of the losses of each individual component between a transmitter and receiver including fiber, couplers and other optical devices and splices. The losses are relative to the transmitter output power and influences the required receiver input power. Power margin,  $P_{MA}$ , represents the amount of power available after deducting linear and nonlinear span losses from the power budget (Ng et al. 2010)

$$\text{Power Budget } (P_B) = \text{Minimum Transmitter Power } (P_{TMIN}) - \text{Minmum Receiver Sensitivity } (P_{RMIN}) \tag{48}$$

$$\text{Link Margin } (P_S) = (\text{Fiber Attenuation} \times \text{Km}) - (\text{Splice Loss} \times \text{No. Splices}) + (\text{Connector Loss} \times \text{No. Connectors}) \tag{49}$$

$$\text{Power Margin } (P_{MA}) = \text{Power Budget } (P_B) - \text{Link Margin } (P_S) - \text{Safety Margin} \tag{50}$$

Fiber link loss dimensions must be given out utilizing a laser source and a power meter in both ways on each fiber span to insure that the original network loss is less than the budgeted loss. In this design, the minimal transmitter power and minimal receiver sensitivity is set as 0 and - 44 dBm. The possible power or power budget for the constructed plan is 44 dBm For performance estimates it is taken up to have signal mux/demux loss  $L_{mux}$  and  $L_{demux}$  ( $\leq 3.5$  dB), contiguous channel other loss  $L_{demux; contiguous}$  (typically > 30 dB), and non-contiguous-channel additional loss  $L_{demux; non-contiguous}$  (typically > 35 dB) (Monroy and Tangdiongga 2002).

Here is the calculation OPB:

$$\text{Power Budget} = T_x \text{ Power} - R_x \text{ Sensitivity} - L \text{ Losses} \tag{51}$$

$$T_x \text{ Power} = 0 \text{ dBm}$$

$$R_x \text{ Sensitivity} = -44 \text{ dBm}$$

$$\text{Losses} = (8\text{-channel Multiplexer/Demultiplexer1 loss}) + (8\text{-channel Multiplexer/Demultiplexer2 loss}) = 38 \text{ dB} \tag{52}$$

$$\text{OPB} = T_x \text{ Power} - R_x \text{ Sensitivity} - \text{Losses} = 0 \text{ dBm} - (-44 \text{ dBm}) - 38 \text{ dB} = 6 \text{ dB} \tag{53}$$

### 5.5 Maximum link distance calculations in DWDM FSO network

After checking the power budget for OF link, we can apply the amount to determine the maximum distance that the network can support. The estimation equation is presented as below.

$$\text{Power Budget} = \text{Buffer Distance} / \text{Fiber Attenuation} \tag{54}$$

Then we will determine the maximum supported distance of FSO link. Here we have the amount for the OF attenuation in Table 2 (0.2 dB/km). The distance is:



$$\text{Distance} = (6 \text{ dB} - 2 \text{ dB}) / 0.2 \text{ dB/km} = 20 \text{ km} \tag{55}$$

### 5.6 Outage probability

The Outage Probability (OUP) is thus achieved by summing the collective pdf around the region that the BER of target is smaller than the instantaneous BER (InstBER) and is given as (Aladeloba et al. 2012a, b, c, 2013; Mbah et al. 2017)

$$P_{OUT}(I_d, I_l) = \int \int_{R_x} p_{X_d, X_l}(I_d, I_l) \langle I_d \rangle, \langle I_l \rangle dI_d dI_l \tag{56}$$

where  $R_x$  is the region in  $(I_d, I_l)$  space where  $BER_{inst}(I_d, I_l) > BER$  target. Equation (56) could be simplified further as (Mbah et al. 2014, 2017),

$$P_{OUT}(\langle I_d \rangle, \langle I_l \rangle) = \int_0^\infty \int_0^{I_{dt}(I_l)} p_{X_d}(I_d, \langle I_d \rangle) p_{X_l}(I_l, \langle I_l \rangle) dI_d dI_l = \int_0^\infty p_{X_l}(I_l, \langle I_l \rangle) \left[ \int_0^{I_{dt}(I_l)} p_{X_d}(I_d, \langle I_d \rangle) dI_d \right] dI_l \tag{57}$$

where the threshold instantaneous of irradiance  $I_{dt}(I_l)$  is required to obtain a  $BER_{inst}$  equals to the BER purpose and is rely on the interferer spontaneous irradiance. The system instantaneous BER is dependent on the interferer and instantaneous irradiances of the signal  $(I_d, I_l)$  (Aladeloba et al. 2012a, b, c),

$$BER_{inst}(I_d, I_l) = \frac{1}{4} \operatorname{erfc} \left( \frac{Q(I_d, I_l)}{\sqrt{2}} \right) \tag{58}$$

$$Q(I_d, I_l) = \frac{i_{1,0}(I_d, I_l) - i_{0,1}(I_d, I_l)}{\sigma_{1,0}(I_d, I_l) + \sigma_{0,1}(I_d, I_l)} \tag{59}$$

### 6 Numerical results and discussion

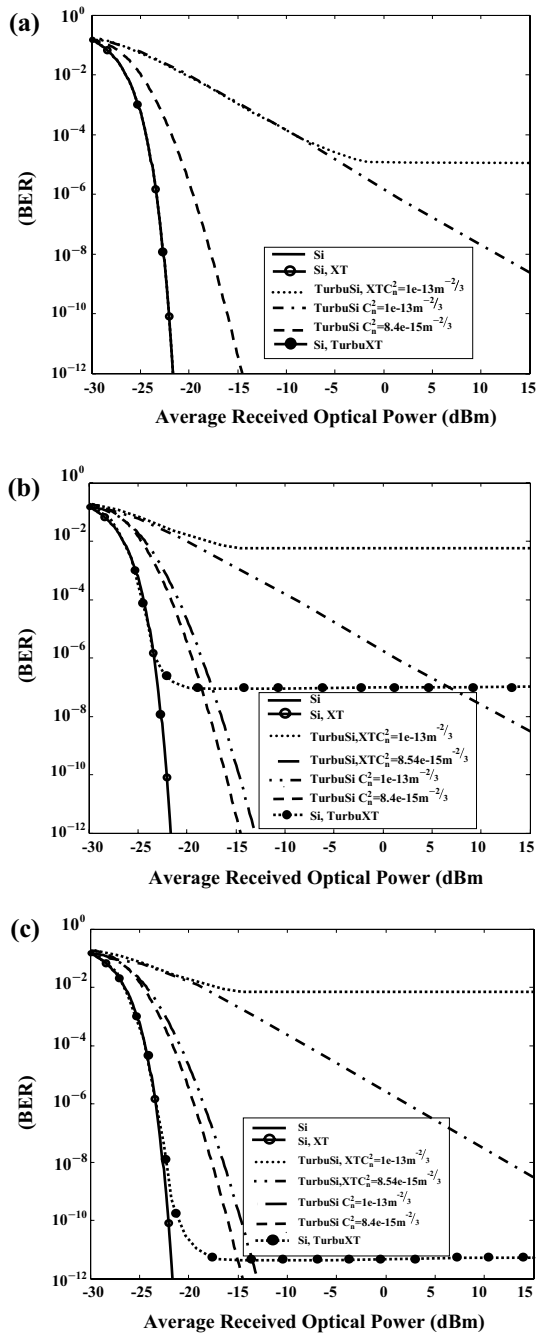
Power penalty, BER required OS transmission power results are performed utilizing specifications reported in Table 2. DPPM COL with  $M=2$  is used for all computations to control the bandwidth extension down while yet retaining the attractive qualities of DPPM. The required optical power applied to in this work represents the transmitter power at the OLT for DTS and ONU for UTS power of 20 dBm is deemed reliable for FSO transmission system around the 1550 nm wavelength region. Refractive index structure constant ranging from  $C_n^2 = 1 \times 10^{-17}$  to  $1 \times 10^{-13} \text{ m}^{-2/3}$  are used for FSO link length of 0–2500 m, corresponding to RVAR ( $\sigma_R^2$ ) range of 0 to 10.6811 and covering all the AT regimes. Aperture Averaging (AA) is integrated in the turbulence model for scintillation mitigation through the operation of Eqs. (2) and (3). Amplifier concentration-based implements, fiber dispersion, and other non-linearities are ignored in the analysis, and a proper extinction ratio is assumed for the OOK calculations. Results in terms of AROP are given to conclude the behavior for different schemes of DWDM FSO system. The TRNVAR  $\sigma_{th-OOK}$  with

$R_b = 2.5$  Gbps is back determined employing the DPPM bandwidth using the DPPM bandwidth extension factor  $B_{\text{exp}} = 2^M/M$  (Sibley 1995) and  $\sigma_{\text{th-DPPM}}^2 = B_{\text{exp}} \sigma_{\text{th-OOK}}^2$ . The thermal noise current is taken as  $(7 \times 10^{-7} \text{ A})$  with sensitivity  $-23$  dBm at BER of  $10^{-12}$  (Ramaswami and Sivarajan 2002). For the calculation, we assume that the bandwidth for the multiplexer/demultiplexer channel bandwidth is 60 GHz, with 3.5 dB insertion loss and a contiguous channel spacing of 100 GHz in the C-band of the ITU (International Telecommunication Union) Grid Sector. Numerical results are presented the analysis of ICC for all the cases (1) No Interferer, No AT Si); (2) Signal with AT, No Interferer (TurbuSi); (3) Signal with AT, Interferer with No AT (TurbuSi,XT); (4) Signal with Interferer, No AT (Si,XT); and (5) Signal with No AT, Interferer with AT (Si, TurbuXT). The WT and ST conditions for FSO link length  $l_{\text{fso}} = 1000$  m come from  $C_n^2 = 8.4 \times 10^{-15} \text{ m}^{-2/3}$  and  $C_n^2 = 1 \times 10^{-13} \text{ m}^{-2/3}$ , respectively. We considered an optically preamplified receiver without any other losses, to clearly the effects of crosstalk alone.

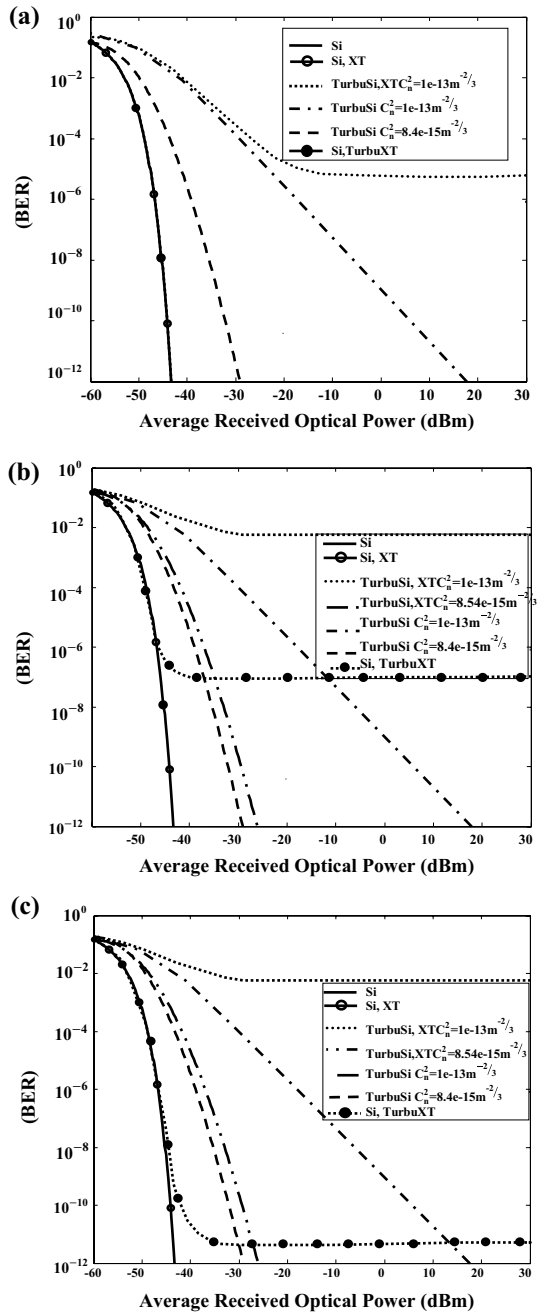
Figure 2 depicts the results of our calculations with the analysis AT that accentuated ICC [present]. As one can see in Fig. 2, BER versus average received optical power (dBm) for AT regimes with no amplifier when (a)  $C_{\text{XT}} = 30$  dB (Aladeloba et al. 2013), (b)  $C_{\text{XT}} = 15$  dB [present] and (c)  $C_{\text{XT}} = 25$  dB [present]. The Error Floor (EF) that occurs in the case of Si, TurbuXT because the demux Contiguous Channel Rejection Ratio (CCRR)  $L_{\text{demux,XT}}$  reduced the power of turbulent interferer. The ER starts once the SIGP and CXTP are sufficiently high that the noises are very unlikely to cause a reverse threshold crossing. In Fig. 2 shows all the cases of BER floors, in the ST cases the TurbuSi,XT BER floors when  $C_{\text{XT}} = 30$  dB, and while in WT the TurbuSi,XT and Si,TurbuXT both EF when  $C_{\text{XT}} = 15$  dB and  $C_{\text{XT}} = 25$  dB that rises with Turbulence Strength (TS), [present]. For illustration, in Fig. 2a with  $C_{\text{XT}} = 30$  dB shows EF TurbuSi,XT with  $C_n^2 = 1 \times 10^{-13} \text{ m}^{-2/3}$  in ST cases while the TurbuSi,XT and Si,TurbuXT both error floor when  $C_{\text{XT}} = 15$  dB as shown in Fig. 2b. Also, when  $C_{\text{XT}} = 25$  dB shows both the EF TurbuSi,XT and Si,TurbuXT but in the Si,TurbuXT case occurs at much lower BERs for WT as seen in Fig. 2c.

Figure 3 shows BER versus average received optical power (dBm) for turbulence regimes with an amplified case when (a)  $C_{\text{XT}} = 30$  dB (Aladeloba et al. 2013), (b)  $C_{\text{XT}} = 15$  dB [present] and (c)  $C_{\text{XT}} = 25$  dB [present]. The Crosstalk XT effects is small without AT (as shown by the Si,TurbuXT BER curves in Fig. 3a and b and c) where the dependencies BER on AROP for all the mentioned cases that presented in Aladeloba et al. (2013) where in Fig. 3b with  $C_{\text{XT}} = 15$  dB, the EF at BER of  $10^{-7}$  and in Fig. 3c  $C_{\text{XT}} = 25$  dB shows the EF at considerable lower BER of  $10^{-11}$  [present]. To understand the EF of AT ICC, the case of Si,TurbuXT can increase to 1 value so {crosstalk become 1, data 0} is greater than {crosstalk 0, data 1} when  $h_{\text{int}}$  is higher from  $h_{\text{sig}}$ , when value a data rate is faster from turbulence leading to EF this occur when  $h_{\text{int}} > h_{\text{sig}}$ . In the case of TurbuSi,XT same case Si,TurbuXT except POP attenuation of the signal. The EF occurs when AT has increased the interfering  $h_{\text{int}} > h_{\text{sig}}$ . FEC can bring about much better performance. Note, however, that the actual link between the LTAS power BER before and after the FEC would require the FEC to enter the analysis. FEC would improve largely the procedure in handling with EF and increasing the feasible target BER. Times of CXTP is huger than the SIGP leads to the turbulent, there is a perfect detection of crosstalk of BER for the signal, so the error floor is easily provided by  $0.5 \times \text{prob}(CXTP > SIGP)$ . The BER use where the EFs occur is thus worked out by both the TS and the demux Channel Rejection Ratio (CRR) (which precisely deals with the CXTP). Before the error floors occur, the process BER operation is defined by turbulence (ASEBN, ASEN, ASE-shot etc.) and an increase in the Signal-to-Noise-Ratio (SNR) of the system improves the BER. Similarly, at low power, the influences the signal and worsens BER. Turbulent conditions considered

**Fig. 2** BER versus average received optical power (dBm) for ST and WT with (no amplifier) **a**  $C_{XT} = 30$  dB (Aladeloba et al. 2013), **b**  $C_{XT} = 15$  dB [present], **c**  $C_{XT} = 25$  dB [present]



**Fig. 3** BER versus average received optical power (AROP) (dBm) for ST and WT (with amplifier) ( $G = 30$  dB) **a**  $C_{XT} = 30$  dB (Aladeloba et al. 2013), **b**  $C_{XT} = 15$  dB [present], **c**  $C_{XT} = 25$  dB [present]



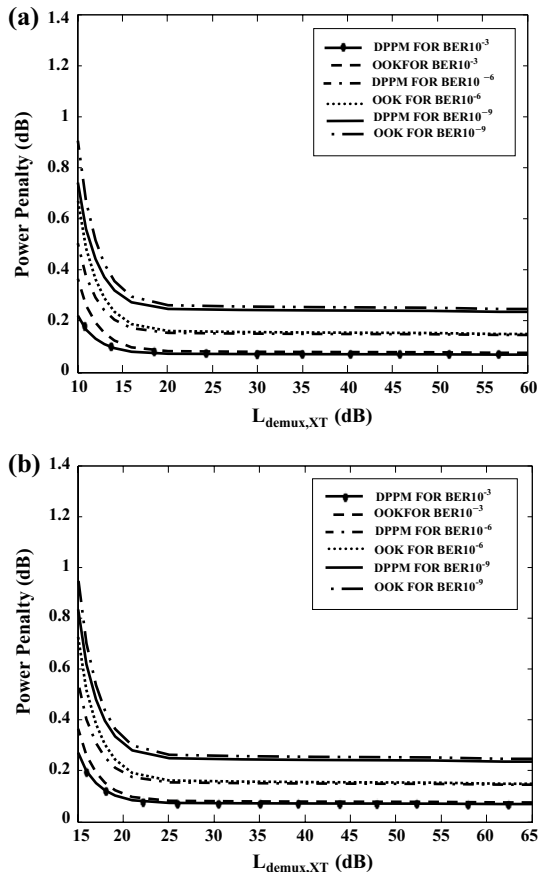
are  $C_n^2 = 1e - 17 m^{-2/3}$ ,  $C_n^2 = 1e - 15 m^{-2/3}$ , and  $C_n^2 = 1e - 13 m^{-2/3}$ . If the resulting  $\sigma_R^2 < 1$ , we have WT; if  $\sigma_R^2 \approx 1$ , we have moderate and if  $\sigma_R^2 > 1$ ; we have ST.

Figure 4 shows the PP (dB) for a interferer demux CRR  $L_{demux,XT}$  at  $l_{fso} = 1500$  m and  $C_n^2 = 1e - 16 m^{-2/3}$  which presented in Mbah et al. (2016), (b) interferer demux channel rejection  $L_{demux,XT}$  at  $l_{fso} = 2000$  m and  $C_n^2 = 1e - 17 m^{-2/3}$  [present]. Figure 4a shows

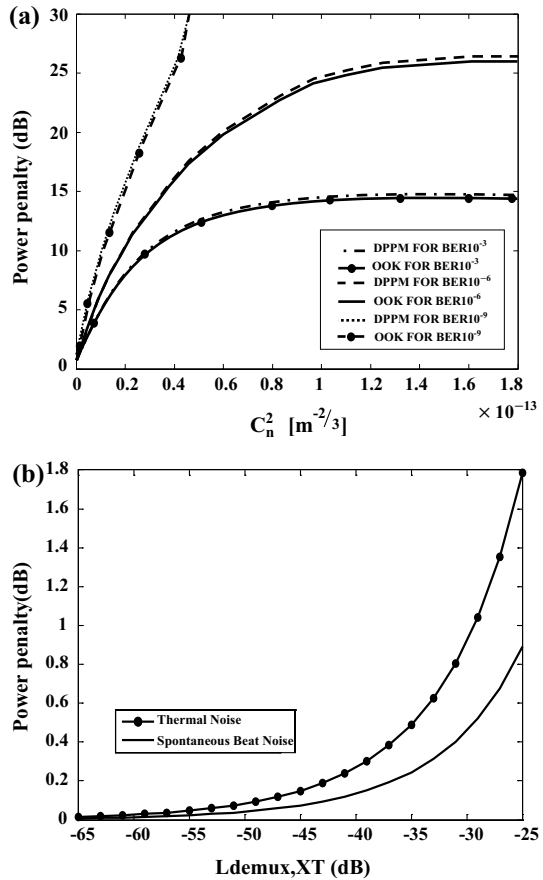
the DPPM PP about of 0.2 –0.7 dB for WT are reported for BER about  $10^{-3} - 10^{-9}$ , respectively of  $C_n^2 = 1e - 16 m^{-2/3}$  and  $l_{fso} = 1500$  m which is presented in Mbah et al. (2016), while in Fig. 4b shows the PP for the OOK system be upper than DPPM for WT with  $C_n^2 = 1e - 17 m^{-2/3}$  and  $l_{fso} = 2000$  m where the DPPM PP about 0.2 –0.8 dB at BER about  $10^{-3} - 10^{-9}$  for WT, respectively [present] while the OOK about 0.3 –1.0dB at BER about  $10^{-3} - 10^{-9}$  for WT. Comparing Fig. 4a, b we show the enhancement of the PP from  $l_{fso} = 1500$  to 2000 m at 0.2 –0.8 dB of BER about  $10^{-3} - 10^{-9}$  for WT, respectively. The proposed approach of DPPM merges higher enhancement of PP about 0.8 dB for BER  $10^{-9}$  at distance 2000 m compared to OOK at 1 dB for WT [present].

Figure 5 shows the PP (dB) for a the UTS as a function of  $(C_n^2 m^{-2/3})$ , with  $(L_{demux,XT} = 35$  dB ) b interferer demux CRR  $(L_{demux,XT})$ . Figure 5a shows the OOK is lower PP compared to the DPPM modulation under MT to ST. As shown in Fig. 5a with NINT of the DPPM PP is greater than the OOK by 0.2 dB and increasing to 0.5 dB as the TS. OOK requires lower PP than DPPM for all values of  $C_n^2 = 1e - 13 m^{-2/3}$ . The DPPM sensitivity has been reduced over OOK systems in the presence of AT as given in Aladeloba et al. (2012a, b, c), without interferers. The distinction between the PP of both systems is reduction of turbulence in the existence of interferers. We use the Power Control (PC) from the RN to monitor and control of the OLT with estimation each ONUs distance from the RN in order to determine the required transmit power from such distance to

**Fig. 4** Power penalty (PP) (dB) versus a  $L_{demux,XT}$  at  $l_{fso} = 1500$  m and  $C_n^2 = 1e - 16 m^{-2/3}$  which presented in Mbah et al. (2016), b  $L_{demux,XT}$  at  $l_{fso} = 2000$  m and  $C_n^2 = 1e - 17 m^{-2/3}$  [present]



**Fig. 5** Power penalty (dB) for **a** the upstream as function of the refractive index structure constant ( $C_n^2 m^{-2/3}$ ) at  $L_{\text{demux,XT}} = 35$  dB, **b** interferer demux channel rejection ratio (CCR) ( $L_{\text{demux,XT}}$ ) (dB)



achieve the defined quality of service (QoS). In implementing PC, the system determines the required transmitter power ( $P_{\text{TXmin}}$ ) independent of the net link path loss to achieve the set QoS or BER. Figure 5b shows the CRR loss ( $L_{\text{demux,XT}}$ ) (dB) versus the PP. In this section, it has been provided a methodology for calculating the PP side by side in the presence of the Dominant Signal Noise (DSN) dependent noise has been presented (Phillips 2007). It can be seen in Fig. 5b, the PP that dominated by thermal noise higher than the PP signal received from thermal noise. Signals received at each station of the system and two cases, this means that the PP of each case also has different values depending on the situation, when the DSN and spontaneous noise when the signal is dominated by a different PP. Using a mathematical model, the results shown in Table 4.

The curves DTS BER appears for a Single Interferer (SINT) as both ST and WT is shown in Fig. 6 of the signal and interferer FSO link lengths of 2500 m. Figure 6 shows that the DTS required OP (dBm) (BER of  $10^{-6}$ ) as a function of the length of the link FSO (a)  $L_{\text{demux,XT}} = 30$  dB, (b)  $L_{\text{demux,XT}} = 15$  dB,  $l_{\text{fso}} = 2500$  m with OOK and DPPM for the No Interferer (NINT) and SINT cases. For Case A, with signal and crosstalk transmit same the powers. In Fig. 6a both the NINT and SINT cases have very similar to the transmission power required as a result of the high signal to crosstalk ratio (and no AT-ICC). The result of Fig. 6, its coverage of all turbulent cases from weak to moderate and

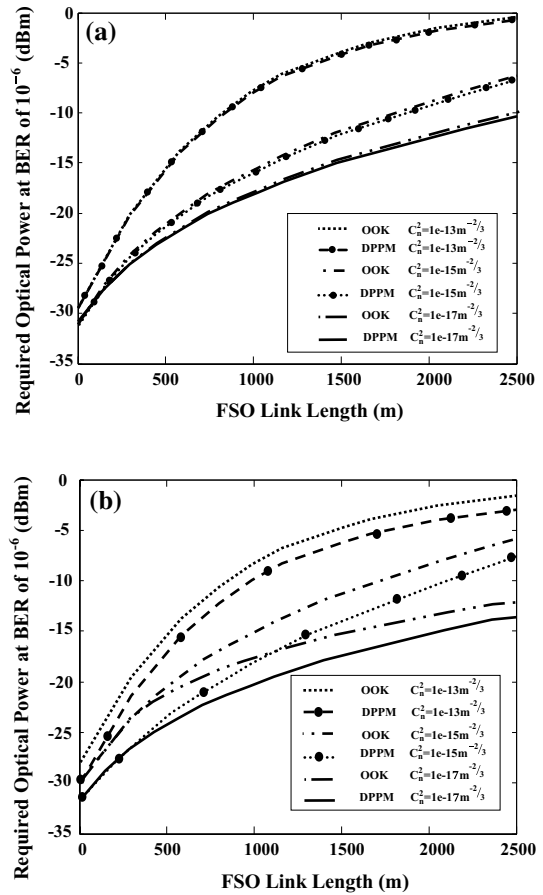
strong turbulence. In the case of strong turbulence  $C_n^2 = 1 \times 10^{-13} \text{ m}^{-2/3}$ , and increasing the AROP. In Fig. 6a, the interferer demux rejection is 30 dB and both SAI are at the same distance from the RN. Numerical result shows that the downstream AROP (dBm) at BER of  $10^{-6}$  in OOK is higher from DPPM. Also in Fig. 6 shows AROP increased with the  $C_n^2$  and FSO link length. Generally, as the FSO link length increases, the AROP increases, since the attenuation, scattering, beam losses spreading and scintillation increase, when  $C_n^2 = 1 \times 10^{-13} \text{ m}^{-2/3}$ . For first case, the NINT and SINT transmitted power in same time, for second case that the NINT and SINT transmitted with high  $C_{XT}$  to obviate the effects AT accentuated ICC seen Fig. 6a. Figure 6b shows the crosstalk effect becomes noticeable, though not dramatically (Aladeloba et al. 2013) and  $L_{\text{demux,XT}} = 15 \text{ dB}$  is lower demux or indigent demux. From Fig. 6, if the power was transferred to be a high value as 0 dBm, it can overcome the effects of turbulence for all systems are considered except  $C_n^2 = 1 \times 10^{-13} \text{ m}^{-2/3}$  and  $l_{\text{fso}} > 1500\text{m}$  in case of the single interferer. In Fig. 6, if the  $T_x$  was fixed OLT power in the 0 dBm (to reduce non-linear fiber), it can be used to infer FSO link lengths of about 1500 m can be used for the case of ST condition. In Case B, amplifiers placed at the OLT transmitter quite similar results not shown are obtained in Case A, above due to the low loss of fiber. However, for Case B is low allowed transmitter about  $-10 \text{ dBm}$  (Ramaswami and Sivarajan 2002) due to the integrity of the fiber. RVAR  $\sigma_R^2$  is constant for a specific curve and the  $T_x$  power for the SAI are supposed to be the same, so only the demux CCRR loss ( $L_{\text{demux,XT}}$ ) is accountable for the crosstalk. The effect of crosstalk is seen to be small without turbulence even for a demux with poor CCRR (15 dB).

Figure 7 shows the UTS required transmitted OP (dBm) (BER of  $10^{-6}$ ) as a function of the FSO link length (a)  $L_{\text{demux,XT}}=30 \text{ dB}$ , (b) transmitter divergence angle  $\theta_{\text{XT}}=0.2 \text{ mrad}$ ,  $l_{\text{fso}}=2500 \text{ m}$  with OOK and DPPM for the no interferer and SINT cases. The result of Fig. 7 covered for all the cases in turbulent from WT to MT and ST. Figures 6a and 7a, it can be seen that the required transmit power is higher in the UTS case by about 7 dBm when  $C_n^2 = 1 \times 10^{-13} \text{ m}^{-2/3}$  and  $l_{\text{fso}} = 2500$ . The results show that the UTS required transmitted optical power (dBm) at BER of  $10^{-6}$  in OOK is higher from DPPM. Demux CCRR values typically  $\leq -15 \text{ dB}$  and  $\geq -45 \text{ dB}$  have been investigated in Yu and Neilson (2002), Maru et al. (2007), Hirano et al. (2003) and are considered. Thus, it is remarkable for a good designer of PON to determine the closest distance to the RN each ONU should be in order to achieve the required system performance with appropriate consideration to the demux CCRR  $L_{\text{demux,XT}}$ . For example, using a  $L_{\text{demux,XT}}$  of 30 dB as seen in Fig. 7a when the user interfering is 1000 m from the RN required and then the required ONU cannot

**Table 4** Numerical results when the signal is dominated by a different power penalty

$L_{\text{demux,XT}}$		Power penalty	
Signal dominated by thermal noise	Signal spontaneous beat noise dominated	Signal dominated by thermal noise	Signal spontaneous beat noise dominated
-35	-35	0.49	0.245
-33	-33	0.6264	0.3132
-31	-31	0.8045	0.4023
-29	-29	1.04	0.5198
-27	-27	1.355	0.6775
-25	-25	1.787	0.8938

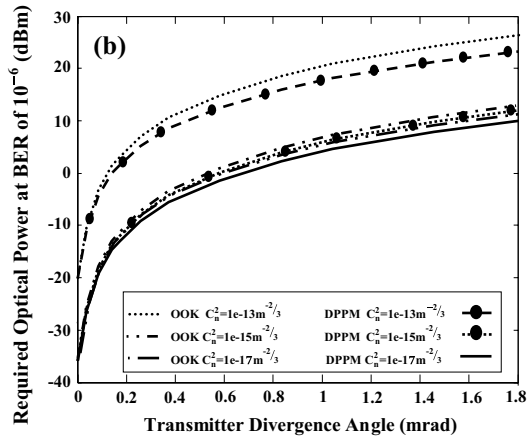
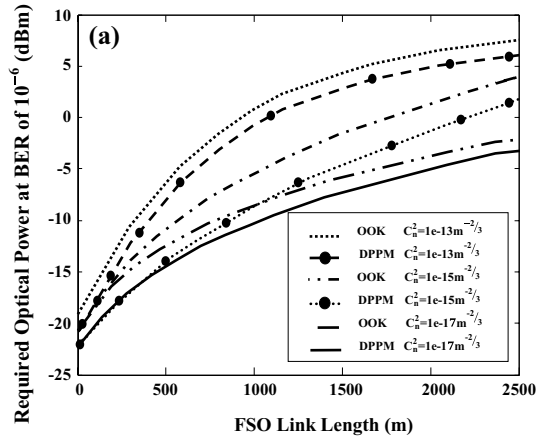
**Fig. 6** Downstream required optical power (dBm) at target BERs of  $10^{-6}$  for ST and WT as function of the FSO link length (m) for no interferer and single interferer cases, **a**  $L_{\text{demux, XT}} = 30$  dB, **b**  $L_{\text{demux, XT}} = 15$  dB



be more than 1500 m ONU of RNs for the target BER to be met at all regimes for WT, MT and ST. To avoid some of the problems of AT, may be included PC algorithm in the system to monitor each ONU power transmission relative to the distance from the RN provides that the same receptor is the ability to RCL for each user, as shown in the design. If the ONU is required in the 2500 m away from the RN mode, and then for another ONU interferer to be in the 1000 to RN, a demux with CCR higher than 45 dB is required so that the target BER is reached for all turbulence regimes as seen in Fig. 7a. The ONU transmits power can be up to 10 dBm to fulfill the eye-safety condition for a C-band wavelength range (Aladeloba et al. 2013; Mbah et al. 2016). When the TxDA ( $\theta_{XT}$ ) and the  $C_n^2$  increases since the AROP clearly increased as shown in Fig. 7b. The non-tracking with the transmission beam of relatively large differences  $\theta_{XT}$  for  $> 1$  mrad, more powerful than the tracking systems will be required. For the automatic pointing and tracking, the system with  $\ll 1$  mrad to be narrow and allow with the pointing and tracking for safely collecting a large proportion of the transmitted energy. It can provide information about the location of the receiver. The tracking system is also pointing jitter errors (Aladeloba et al. 2012a, b, c) not included here. To achieve a BER of  $10^{-6}$  and  $I_{\text{fso}}$  of 1500 by using small transmission divergence angle (about 0.12 mrad). The results show the impact of ICT on the UTS through the evaluation of BER versus AROP (dBm) within the transmission distance of 2500 m with



**Fig. 7** Upstream required optical power (dBm) at target BERs of  $10^{-6}$  for ST and WT at  $L_{\text{demux,XT}} = 30$  dB **a** as function of the FSO link length (m) for no interferer and single interferer cases, **b** transmitter divergence angle  $\theta_{\text{XT}} = 0.2$  mrad with  $l_{\text{fso}} = 1500$  m

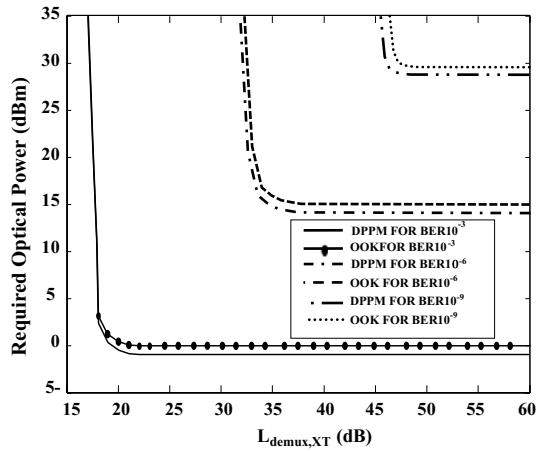


$L_{\text{demux,XT}} = 30$  dB, for different FSO link lengths from the interferer to the RN  $d_{\text{int}}$ , using good demux ( $L_{\text{demux,XT}} = 30$  dB). If a good demux device is used Fig. 7 at  $\text{BER} = 10^{-6}$ , the effect of crosstalk is negligible as AROP stays the same in both cases of  $d_{\text{int}} = d_{\text{sig}}$ .

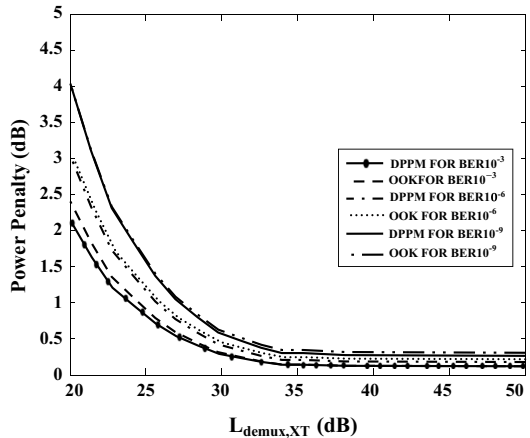
Figure 8, shows the required OP (dBm) for the UTS as a function of RINS constant ( $C_n^2 m^{-2/3}$ ) and interferer demux channel rejection  $L_{\text{demux,XT}}$  (dB) at  $l_{\text{fso}} = 2000$  m. The result as for target BERs concerning  $10^{-9}$ ,  $10^{-6}$ , and  $10^{-3}$ , in accordance with remain met at entire AT regimes, the system requires demux with a CRRR better or equalize in accordance with 46 dB, 33 dB, and 17 dB, respectively. However, to get a BER regarding  $10^{-9}$  would need great OP (above 25 dB). FEC carried out between most recent realistic systems, function at BER about  $10^{-3}$  is becoming appropriate and demultiplexers along 18 dB rejection is effortlessly available.

Figure 9 shows the PP (dB) for the UTS as a function of the RINS constant ( $C_n^2 m^{-2/3}$ ) at  $C_n^2 = 1e - 17 m^{-2/3}$  and interferer demux CRR  $L_{\text{demux,XT}}$  (dB) at  $l_{\text{fso}} = 250$  m. The result shows that the PP for the DPPM system tends in conformity with keep lower than that on the OOK system. Obtained results in Fig. 9 shows that the PP for DPPM about 2.0 – 3.0 dB and 2.0 – 4.0 dB for WT are reported of BER about  $10^{-3} - 10^{-6}$  and  $10^{-3} - 10^{-9}$ , respectively. As shown in Fig. 9, an interferer that is closer to the RN more crosstalk to other users

**Fig. 8** Required optical power (dBm) for the upstream as a function of the refractive index structure constant (RINS) ( $C_n^2 m^{-2/3}$ ) and interferer demux channel rejection  $L_{demux,XT}$  (dB) at  $l_{iso} = 2000$  m



**Fig. 9** Power penalty (dB) for the upstream as a function of the refractive index structure constant ( $C_n^2 m^{-2/3}$ ) at  $C_n^2 = 1e - 17$  m<sup>-2/3</sup> and interferer demux channel rejection  $L_{demux,XT}$  (dB) at  $l_{iso} = 250$  m



further away, even at below value ( $C_n^2 m^{-2/3}$ ). Thus, in the non-attendance of PC, user stationing should be dealt with as an essential design specification.

Figure 10 shows the result of OUP in the existence of a single turbulent interferer for a DWDM FSO OOK system compared to a situation where there is no interferer. The system outage offers with different RINS ( $C_n^2$ ), demultiplexer CCRR ( $L_{demux,XT}$ ) and RL aperture diameter are examined for an FSO channel length ( $l_{iso}$ ) of 2000 m for both SAI. With the presence of the interferer, outage floors analogous to the EFs obtained for BER evaluations in Aladeloba et al. (2013), Mbah et al. (2016) occur where the floor position shifts with change in  $C_n^2$  and  $L_{demux,XT}$  respectively in Fig. 10a, b. Figure 10c shows that AA which is a commonly used AT mitigation technique (Vetelino et al. 2007) improves the OUP of the system. As seen in Fig. 10c, increasing the RL aperture diameter from 1.55 to 2.55 cm decrease the OUP of the system with turbulence-affected interferer from 10<sup>-6</sup> to about 10<sup>-9</sup> at about 27 dBm/cm<sup>2</sup> mean irradiance.

To further support up this point, in Fig. 11, we show a plot concerning the Required Mean Irradiance (RMI) to obtain InstBER overall performance target about 10<sup>-6</sup> then 10<sup>-3</sup> with including fixed OUP values regarding both 10<sup>-6</sup> or 10<sup>-3</sup> and RMI to achieve average BER aims regarding of 10<sup>-6</sup> and 10<sup>-3</sup> for a DWDM FSO system (Mbah et al.

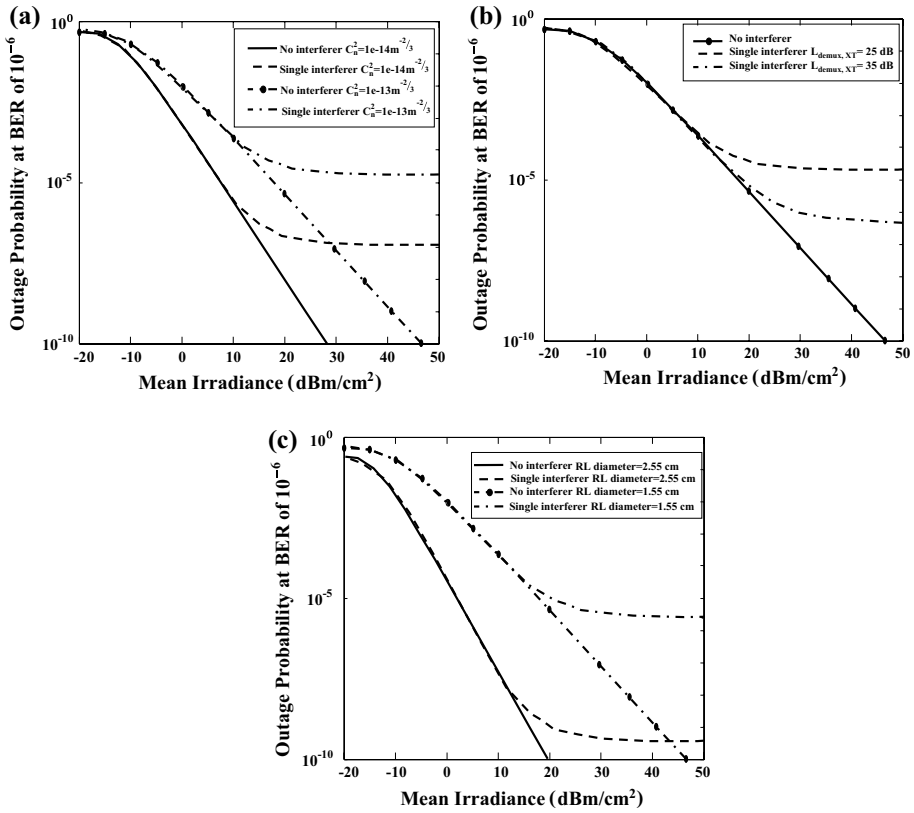
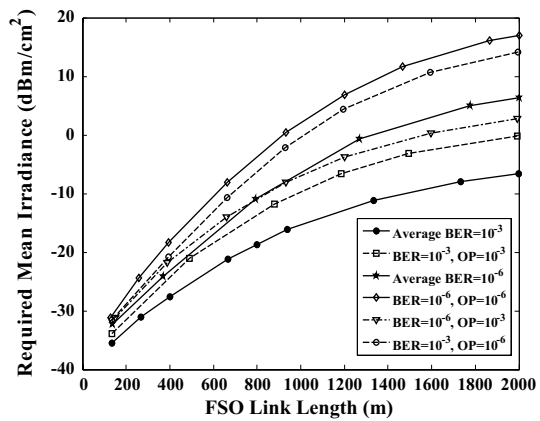


**Fig. 10** Outage Probability (OUP) versus Mean Irradiance for a turbulent system (FSO link length=2000 m) **a** for different values of  $C_n^2$  at  $L_{\text{demux,XT}} = 35$  dB, **b** for different values of  $L_{\text{demux,XT}}$  at  $C_n^2 = 1 \times 10^{-13} \text{ m}^{-2/3}$ , **c** for different values of RL aperture diameter at  $L_{\text{demux,XT}} = 35$  dB and  $C_n^2 = 1 \times 10^{-13} \text{ m}^{-2/3}$ . (Reproduced with permission from Mbah et al. 2016)

**Fig. 11** Required Mean Irradiance (RMI) as a function of the FSO link length to achieve instantaneous BER targets with fixed Outage Probability (OUP) values and average BER targets at  $L_{\text{demux,XT}} = 35$  dB and  $C_n^2 = 1 \times 10^{-13} \text{ m}^{-2/3}$



2017). From the end results proven of Fig. 11 it is seen that with  $L_{\text{demux,XT}} = 35$  dB and  $C_n^2 = 1 \times 10^{-13} \text{ m}^{-2/3}$ , the RMI to attain a target InstBER of  $10^{-6}$  with OUP target of  $10^{-3}$  for all links of FSO transmission considered. This shows so extra transmitter power is required according to enhance OUP for a given a partial InstBER target than in accordance with enhance the InstBER a given OUP target. This shows that the transmitter power more is required to improve the OUP for a given InstBER target than to improve InstBER for a specified OUP target. From the result shown in Fig. 11 it is seen that with  $L_{\text{demux,XT}} = 35$  dB a and  $C_n^2 = 1 \times 10^{-13} \text{ m}^{-2/3}$ , the RMI to obtain a target InstBER of  $10^{-3}$  with OUP target of  $10^{-6}$  is greater than RMI to achieve a target InstBER of  $10^{-6}$  with OUP target of  $10^{-3}$  for all FSO lengths considered (Mbah et al. 2017). This shows that more transmitter power is required to improve OUP for a given InstBER target than to improve the InstBER for a given OUP target. For example, at 2000 m in Fig. 11, extra 2.66 (dBm/cm<sup>2</sup>) is required to improve the instantaneous BER from  $10^{-3}$  to  $10^{-6}$  at fixed OUP of  $10^{-3}$ , while it takes additional 14.23 dBm/cm<sup>2</sup> to improve the OUP from  $10^{-3}$  to  $10^{-6}$  at fixed InstBER of  $10^{-3}$ . The values  $\alpha$  and  $\beta$ , are analyzed at  $l_{\text{fso}} = 1000$  m, ( $\alpha = 4.2739$ ), ( $\beta = 3.1606$ ) at  $C_n^2 = 1 \times 10^{-13} \text{ m}^{-2/3}$ , RVAR  $\sigma_R^2 = 1.9910$  and we calculated the total OLT receiver value ( $\sigma_{\text{th}}^2 = 98 \times 10^{-14}$  A) as seen in Fig. 12. The bit is sampled and compared with ADT. For OOK-NRZ signaling assumed here, the Kalman filtering method (Chen et al. 2008) represents a realistic adaptive approach to achieving near the optimal threshold for each instantaneous power level, and such an optimal is assumed. All noises and scintillation due to vulnerability to refractive index fluctuations arising of variation air temperature, pressure (Dar and Jha 2017; Kaushal et al. 2017) are analyzed. The results show BER floors of the interchannel crosstalk are analyzed for WT and ST in this study. Table 5 show the calculations results of  $\alpha$  and  $\beta$  and RVAR  $\sigma_R^2$  at  $l_{\text{fso}} = 1000$  m. Typical values of  $\sigma_R^2$ ,  $\alpha$  and  $\beta$  used for modelling WT, MT, ST and Saturated Turbulence regimes are shown in Table 6 (Ghassemlooy et al. 2013; Andrews and Phillips 2005; Aladeloba et al. 2012a, b, c; Popoola and Ghassemlooy 2009). The PP induced by Multiple Access Interference (MAI) only (i.e. relative to when one ONU is active on the required wavelength) for individual object BER values is shown in Fig. 13. The implement of MAI is less prominent at ST conditions with a maximum PP contribution of about 1 dB when the 8 ONUs are active and at target BER of  $10^{-6}$ . The effect of MAI is more prominent at WT conditions and for  $C_n^2$  of  $1 \times 10^{-16} \text{ m}^{-2/3}$ , a PP of about 6.686 dB is concluded for target BER of  $10^{-9}$  when the 8 user are active on the system of ONUs.

Fig. 12 Gamma–Gamma pdf for our calculations of turbulence regimes

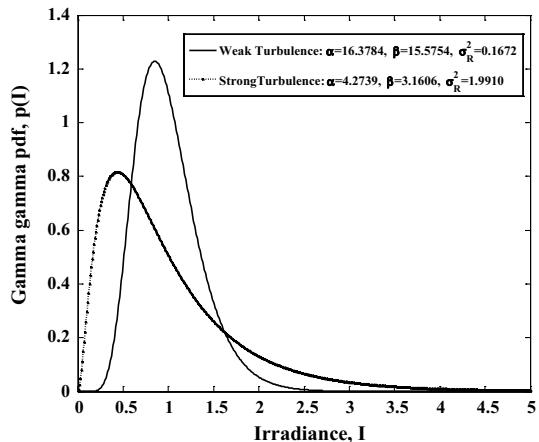


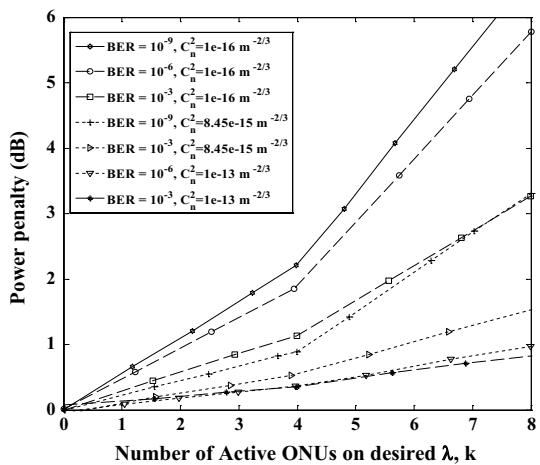
**Table 5** Calculations results of  $\alpha$  and  $\beta$  and RVAR  $\sigma_R^2$  at  $l_{fso} = 1000$  m

Parameters	$\alpha$	$\beta$	$\sigma_R^2$
$C_n^2$ $1 \times 10^{-13} \text{ m}^{-2/3}$	4.2739	3.1606	1.9910
$8.4 \times 10^{-15} \text{ m}^{-2/3}$	16.3784	15.5754	0.1672
$1 \times 10^{-17} \text{ m}^{-2/3}$	1.2561e+004	1.2444e+004	1.9910e-004

**Table 6** Typical parameters for characteristics weak-to-saturated turbulence regimes. (Reproduced with permission from Ghassemlooy et al. 2013; Andrews and Phillips 2005; Aladeloba et al. 2012a, b, c; Popoola and Ghassemlooy 2009)

Parameters	Turbulence regimes			
	Weak ( $\sigma_R^2 < 1$ )	Moderate ( $\sigma_R^2 \approx 1$ )	Strong ( $\sigma_R^2 > 1$ )	Saturated ( $\sigma_R^2 \rightarrow \infty$ )
$\sigma_R^2$	0.2	1.6	3.5	25
$\alpha$	11.651	4.027	4.226	8.048
$\beta$	10.122	1.911	1.362	1.032

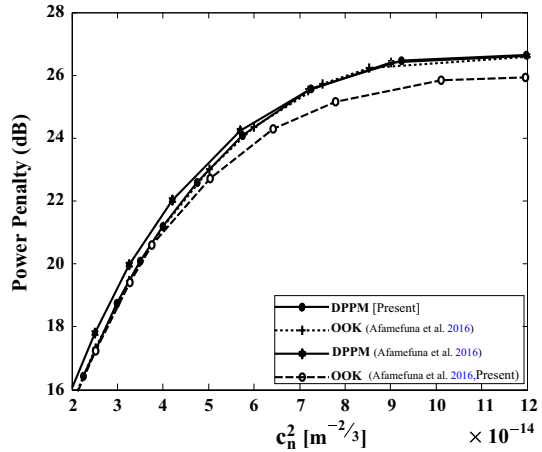
**Fig. 13** Upstream power penalty (dB) for DPPM system for varying  $C_n^2$  and  $L_{demux,XT} = 35$  dB: against number of active ONUs on the desired wavelength with  $l_{fso} = 1500$  m



### 7 Validations

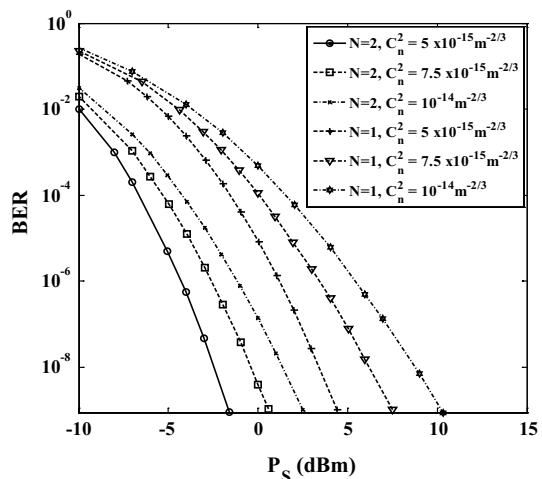
As an analytical approach, it is certain to examine and evaluate the validity of PP results using DPPM and OOK. Figure 14 show PP (dB) for the UTS as a function of RINS ( $C_n^2$ ) at BER of  $10^{-6}$ ,  $l_{fso} = 2000$  m and  $L_{demux,XT} = 35$  dB. Unlike the non-AT WDM DPPM versus OOK crosstalk results in Mbah et al. (2014). For this purpose, we performed the PP results are shown in Fig. 14 that the OOK system has slightly lower PP compared to the DPPM system under moderate-to-ST. The presented result show enhancement of the PP using DPPM at  $l_{fso} = 2000$  m above 20 dB for ST regimes are reported for BER of  $10^{-6}$  as shown in Fig. 14, with no interferer the DPPM PP is greater than the OOK by 0.1 dB, and when the TS increases, the PP reached to 0.5 dB. The difference between the PP of both Mbah et al. (2016) and [present] that the DPPM system tends to be closer to the OOK system at 26.65 dB system. The results show that the DPPM PP is greater than the OOK PP by 0.2 and increase to 0.5 at  $l_{fso} = 1500$  m that presented in Mbah et al. (2016).

**Fig. 14** Comparison of PP (dB) for UTS as a function of the refractive index structure constant ( $C_n^2$ ) at BER of  $10^{-6}$ ,  $l_{fso}=2000$  m and  $L_{demux,XT} = 35$  dB by Mbah et al. (2016, Present)



Next, Fig. 15 illustrates BER of the designed system operating (4-Pulse Position Modulation (PPM) versus  $P_s$ , for the DTS with different turbulence strengths. Within the total distance of 4 km, the BER work is regularly worsened when the when the turbulence becomes stronger (i.e., higher  $C_n^2$ ). With only one relay (N), the required  $P_s$  to attain BER of  $10^{-9}$  are 10.2 dBm, 7.5 dBm, and 4.2 dBm corresponding to  $C_n^2$  of  $10^{-14}m^{-2/3}$ ,  $7.5 \times 10^{-15}m^{-2/3}$ , and  $5 \times 10^{-15}m^{-2/3}$ , respectively [present]. With two relays, the BER performance is significantly improved compared to the case when relay (N=1), the performance improvements when N=2 are 8 dB, 7 dB, and 6 dB for  $C_n^2$  of  $10^{-14}m^{-2/3}$ ,  $7.5 \times 10^{-15}m^{-2/3}$ , and  $5 \times 10^{-15}m^{-2/3}$ , respectively [present]. While N=1, the required  $P_s$  to obtain BER of  $10^{-6}$  are 10.5 dBm, 7.5 dBm, and 4.5 dBm corresponding to  $C_n^2$  of  $10^{-14}m^{-2/3}$ ,  $7.5 \times 10^{-15}m^{-2/3}$ , and  $5 \times 10^{-15}m^{-2/3}$  as published in Trinh et al. (2016). With two relays (N), the BER performance is significantly improved. More specifically, compared to the case when N=1, the performance improvements when N=1, the performance improvements when N=2 are 8 dB, 7 dB, and 6 dB for  $C_n^2$  of  $10^{-14}m^{-2/3}$ ,  $5 \times 10^{-15}m^{-2/3}$ , and  $5 \times 10^{-15}m^{-2/3}$ .

**Fig. 15** Comparison between Downstream transmission: BER versus the average transmitted power per information bit  $P_s$ , with 4-PPM,  $R_b=1$  Gbps,  $L_{demux,XT}=-30$  dB, and  $l_{fso}=4$  km, for different turbulence strengths  $C_n^2m^{-2/3}$  that presented in Trinh et al. (2016, Present)



## 8 Conclusions

A hybrid fiber and DWDM FSO network using OOK and DPPM have been investigated in this paper. The performance evaluation under the impacts of turbulence-accentuated ICC on the system is done. The novel approach of DPPM took advantage to all DWDM HFFSO network and is simple implementation with integrating of hybrid fiber free space optical communication to form a low-cost, flexible, greater bandwidth and huge channel capacity, reliable with higher data rate optical network. The DPPM and OOK scheme at coding level of 2, DPPM gives about 2 dB in required average power over the OOK. Numerical result shows the improvement of the power penalty with OOK and DPPM modulation. The DPPM is a higher power efficient, powerful and results for greater-connection network. These improvements achieved in DPPM format on the price of higher channel bandwidth requires. Depending on the turbulence level, power penalties of 0.2–3.0 dB for WT regimes, and above 20 dB ST regimes are reported for a BER of  $10^{-6}$ . The PP that dictated by thermal noise greater than the power penalty that dominated spontaneous beat noise. The optical received signal spontaneous more accurate than optical received signal by thermal noise. The results of this paper should be appropriate for choosing DPPM modulation to enhancement the PP in DWDM FSO communication. Finally, FEC would further largely the procedure in handling with error floors and correcting the feasible target BER.

**Acknowledgements** Support from University Mansoura, Faculty of Engineering, Electrical Communication Department is gratefully acknowledged.

## Appendix

### This turbulence accentuated interchannel crosstalk effect is considered for the cases are written as Aladeloba et al. (2013)

#### The signal with turbulence but the interferer does not

To do so Eqs. (6–13) are used in an optically preamplified case [gain  $G$ , ASE PSD at the amplifier output], the ASE power spectral density (PSD) is  $N_o = 0.5(NFG - 1)E$  where  $G$  and  $NF$  are the OA gain and noise figure, respectively, with no amplifier ( $G = 1$ ). Then  $P_{R,sig}(h_{sig}) = GP_{inst,sig}(h_{sig})$  where  $P_{inst,sig}(h_{sig})$  is the instantaneous received signal power and thus  $P_{int,sig}(1)$  is also the turbulence-free average received power ( $TrblncFrp_{sig}$ ) of the input signal at the optical preamplifier.  $P_{R,int} = GP_{int}$ , is fixed by setting a signal-to-crosstalk ratio  $C_{XT} = P_{R,sig}(1)/P_{int}$  where  $P_{int}$  is also the crosstalk optical signal power.

#### The interferer experiences turbulence, but not the signal

$P_{R,int}(h_{int}) = GP_{inst,int}(h_{int})$ , where  $P_{inst,int}(h_{int})$  is the instantaneous received interferer power and thus  $P_{R,sig} = GP_{sig}$  is fixed by setting a signal-to-crosstalk ratio  $C_{XT} = P_{sig}/P_{R,int}(1)$ , where  $P_{R,int}(1)$  is also the turbulence-free average received interferer power ( $TrblncFrp_{int}$ ) and  $P_{sig}$  is the (non-turbulent) optical signal power.

## Algorithms

See Table 7.

**Table 7** MATLAB code to calculate the value of (Trb ln cFrP)

```

%% define constants
Rb=2.5*10^9;
mt=2;
eta=1;
c=2.998*10^8;
h=6.626*10^(-34);
lambda=1.55*10^(-6);
r=10;
B0=60*10^9;
Be=Rb/2;
q=1.60218*10^(-19);
G=1;
E=h*c/lambda;
N0=0;
capitalr=eta*q/E;
sigma2shotASE=2*mt*B0*N0*q*capitalr*Be;
sigma2ASEASE=2*mt*(capitalr*N0)^2*B0*Be;
sigma2th=2*49*10^(-14);
prec=[];
lber=[];
for ii=1:1:101
    prec(ii)=-30+(ii-1)*8.3/100;
    p(ii)=10^(-3)*10^(prec(ii)/10);
    sigma2shot1=2*q^2*r/(r+1)*capitalr*p(ii)*Be;
    sigma2shot0=2*q^2/(r+1)*capitalr*p(ii)*Be;
    sigma2sigASE1=4*capitalr*N0^2*r/(r+1)*capitalr*p(ii)*Be;
    sigma2sigASE0=4*capitalr*N0^2/(r+1)*capitalr*p(ii)*Be;
    sigmal=sqrt(sigma2shot1+sigma2sigASE1+sigma2shotASE+sigma2ASEASE+sigma2th);
    sigma0=sqrt(sigma2shot0+sigma2sigASE0+sigma2shotASE+sigma2ASEASE+sigma2th);
    curent0(ii)=2/(r+1)*capitalr*p(ii);
    curent1(ii)=2*r/(r+1)*capitalr*p(ii);
    qq(ii)=(curent1(ii)-curent0(ii))/(sigma0+sigmal);
    arg4ber=qq(ii)/sqrt(2);
    ber(ii)=erfc(arg4ber)/2;
    lber(ii)=log10(ber(ii));
end

% plotting the dependences
hold on
plot(prec,lber,'r');
%axis([20 30 -10^(-1) 10^(-1)])
%set(hPlot, 'LineWidth', 2);
%NF=4.77;
%F=10^(NF/10);
%G=10^(30/10);
%N0=0.5*(F*G-1)*E;
%Lc=1-dblquad('dinteg', 1,1,0,0);
%alfafso=0.0002;
lfso=1000;
%capitalLfso=10^(-alfafso*lfso);
%alfafiber=0.0002;
%lfiber=20000;
%capitalLfiber=10^(-alfafiber*lfiber);
DRX=0.017;
%theta=0.0002;
%capitalLbs=(DRX/(theta*lfso))^2;
%capitalLdemux=10^(0.35);
%capitalLmux=10^(0.35);
%PuTsig=10^(-3)*10^(8/10);
c2n=1.0e-13;
k=2*pi/lambda;
sigmaR2=1.23*c2n*k^(7/6)*lfso^(11/6);
d=sqrt(k*DRX^2/(4*lfso));
alpha=1/(exp(0.49*sigmaR2/(1+0.65*d^2+1.11*sigmaR2^1.2)^(7/6))-1);
beta=1/(exp(0.51*sigmaR2*(1+0.69*sigmaR2^1.2)^(-5/6)/(1+0.9*d^2+0.62*(d^2)*sigmaR2^1.2))-1);
x=[];
Y=[];
x=10^(-12):(10^(-3)-10^(-12))/2000:10^(-3);
precl=[];
lberwtrb=[];
for ii=1:1:101
    precl(ii)=-30+(ii-1)*50/100;
    p1(ii)=10^(-3)*10^(precl(ii)/10);

    %*capitalLfso*capitalLbs*Lc*capitalLmux*capitalLfiber*capitalLdemux);
    for iii=1:1:2001
        hsig(iii)=x(iii)/p1(ii);
    end
end

```



**Table 7** (continued)

```

pgg(iii)=2*(alpha*beta)^( (alpha+beta)/2)/(gamma(alpha)*gamma(beta))*(hsig(iii))^( (alpha+beta)/
2-1)*besselk(alpha-beta, 2*sqrt(alpha*beta*hsig(iii)));
sigma2shot1=2*q*2*r/(r+1)*capitalr*x(iii)*Be;
sigma2shot0=2*q*2/(r+1)*capitalr*x(iii)*Be;
sigma2sigASE1=4*capitalr*N0*2*r/(r+1)*capitalr*x(iii)*Be;
sigma2sigASE0=4*capitalr*N0*2/(r+1)*capitalr*x(iii)*Be;
sigma1=sqrt(sigma2shot1+sigma2sigASE1+sigma2shotASE+sigma2ASEASE+sigma2th);
sigma0=sqrt(sigma2shot0+sigma2sigASE0+sigma2shotASE+sigma2ASEASE+sigma2th);
curent0tub(iii)=2/(r+1)*capitalr*x(iii);
curent1tub(iii)=2*r/(r+1)*capitalr*x(iii);
qq1(iii)=(curent1tub(iii)-curent0tub(iii))/(sigma0+sigma1);
arg4ber=qq1(iii)/sqrt(2);

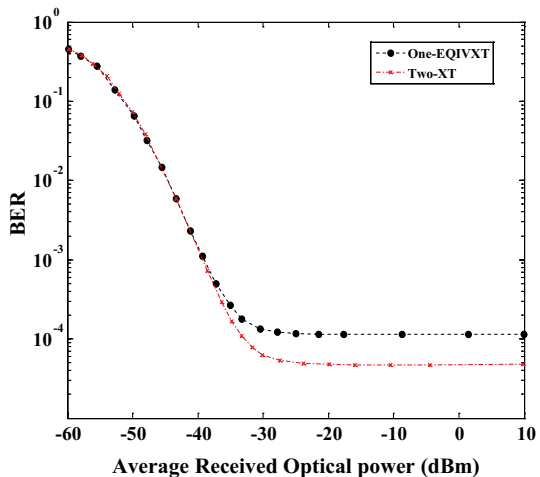
ber1(iii)=erfc(arg4ber)/2; %Lc*capitalLmux*capitalLfiber*capitalLdemux);
y(iii)=pgg(iii)*ber1(iii);
end
berwtrb(ii)=trapz(x, y);
shift=lber(1)-log10(berwtrb(1));
lberwtrb(ii)=log10(berwtrb(ii))+shift;

end
TrblncFrP=10^(-shift)
%ber2(1)=ber1(1)/pgg(1);
%lber2(1)=log10(ber2(1));
%berint=[];
%hsigint=[];
%for ii=2:1:1001
% for iii=1:1:ii
% berint(iii)=ber1(iii);
% hsigint(iii)= hsig(iii);
% end
% ber2(ii)=trapz(hsigint, berint);
% lber2(ii)=log10(ber2(ii));
% end
    
```

**BER comparison of the impact of two crosstalk sources and a single crosstalk source of equivalent power**

See Fig. 16.

**Fig. 16** BER comparison of the impacts of two crosstalk sources and a single crosstalk source of equivalent power in a turbulent FSO DWDM DPPM system with coding level  $M = 2$ ,  $l_{fo,int} = 2000$  m and signal-to-crosstalk ratio  $L_{demux,XT}$  (eprints.nottingham.ac.uk). (Reproduced with permission from Mbah et al. 2014)



## References

- Abtahi, M., Lemieux, P., Mathlouthi, W., Rusch, L.A.: Suppression of turbulence-induced scintillation in free-space optical communication systems using saturated optical amplifiers. *J. Lightw. Technol.* **24**, 4966–4973 (2006)
- Aladeloba, A.O., Phillips, A.J., Woolfson, M.S.: DPPM FSO communication systems impaired by turbulence, pointing error and ASE noise. In: 14th International Conference on Transparent Optical Networks (ICTON), Coventry, UK (2012)
- Aladeloba, A.O., Phillips, A.J., Woolfson, M.S.: Performance evaluation of optically preamplified digital pulse position modulation turbulent free-space optical communication systems. *IET Optoelectron.* **6**(1), 66–74 (2012a)
- Aladeloba, A.O., Phillips, A.J., Woolfson, M.S.: Improved bit error rate evaluation for optically preamplified free-space optical communication systems in turbulent atmosphere". *IET Optoelectron.* **6**(1), 26–33 (2012b)
- Aladeloba, A.O., Woolfson, M.S., Phillips, A.J.: WDM FSO network with turbulence-accentuated inter-channel crosstalk. *OSA/IEEE* **5**(6), 641–651 (2013)
- Aldibbiat, N.M., Ghassemlooy, Z., McLaughlin, R.: Indoor optical wireless systems employing dual header pulse interval modulation (DH-PIM). *Int. J. Commun. Syst.* **18**(3), 285–305 (2005)
- Al-Habash, M.A., Andrews, L.C., Phillips, R.L.: Mathematical model for the irradiance probability density function of a laser beam propagating through turbulent media. *Opt. Eng.* **40**, 1554–1562 (2001)
- Andrews, L.C., Phillips, R.L.: *Laser Beam Propagation Through Random Media*, 2nd edn. SPIE, Bellingham, WA (2005)
- Andrews, L.C., Phillips, R.L., Hopen, C.Y.: *Laser Beam Scintillation with Applications*. SPIE Press, Bellingham, WA (2001)
- Ansari, N., Zhang, J.: *Media Access Control and Resource Allocation for Next Generation Passive Optical Networks*. Springer, Berlin (2013)
- Arnon, S.: Optical wireless communications. In: Driggers, R.G. (ed.) *Encyclopedia of Optical Engineering*, pp. 1866–1886. Marcel Dekker, Inc., New York (2003)
- Badar, N., Jha, R.K.: Performance comparison of various modulation schemes over free space optical (FSO) link employing Gamma-Gamma fading model. *Opt. Quantum Electron.* **49**, 192 (2017). <https://doi.org/10.1007/s11082-017-1025-4>
- Chan, V.W.S.: Free-space optical communications. *IEEE/OSA J. Lightw. Technol.* **24**(12), 4750–4762 (2006)
- Chen, C., Yang, H., Jiang, H., Fan, J., Han, C., Ding, Y. (2008) Mitigation of turbulence-induced scintillation noise in free-space optical communication links using Kalman filter. In: *IEEE Congress on Image and Signal Processing, China, Hainan*, vol. 5, pp. 470–473 (2008)
- Ciaramella, E., Arimoto, Y., Contestabile, G., Presi, M., D'Errico, A., Guarino, V., Matsumoto, M.: 1.28 terabit/s (32×40 Gbit/s) WDM transmission system for free space optical communications. *IEEE J. Sel. Areas Commun.* **27**, 1639–1645 (2009)
- Dar, A.B., Jha, R.K.: Chromatic dispersion compensation techniques and characterization of fiber Bragg grating for dispersion compensation. *Opt. Quantum Electron.* **49**, 108 (2017). <https://doi.org/10.1007/s11082-017-0944-4>
- Dikmelik, Y., Davidson, F.M.: Fiber-coupling efficiency for free-space optical communication through atmospheric turbulence. *Appl. Opt.* **44**(23), 4946–4952 (2005)
- Ghassemlooy, Z., Popoola, W., Rajbhandari, S.: *Optical Wireless Communications—System and Channel Modelling with MATLAB*, 1st edn. CRC Press, London (2013)
- Gyselings, T., Morthier, G., et al.: Crosstalk analysis of multiwavelength optical cross connects. *IEEE J. Lightw. Technol.* **14**, 1423–1435 (1999)
- Hirano, A., Miyamoto, Y., Kuwahara, S.: Performances of CSRZ-DPSK and RZ-DPSK in 43-Gbit/s/ch DWDM G.652 single-mode-fiber transmission. In: *Optical Fiber Communications Conference*, pp. 454–456 (2003)
- Karp, S., Gagliardi, R.M., Moran, S.E., Stotts, L.B.: *Optical Channels: Fibers, Clouds, Water and the Atmosphere*. Plenum, New York (1988)
- Kaushal, H., Jain, V. K., Kar, S.: Free Space Optical Communication, 1st edn. In: *Optical Networks*. (2017). <https://doi.org/10.1007/978-81-322-3691-7>

- Khalighi, M., Schwartz, N., Aitamner, N., Bourennane, S.: Fading reduction by aperture averaging and spatial diversity in optical wireless systems. *J. Opt. Commun. Netw.* **1**(6), 580–593 (2009)
- Killinger, D.: Free space optics for laser communication through the air. *Opt. Photon. News* **13**(10), 36–42 (2002)
- Lee, C.H., Sorin, W.V., Kim, B.Y.: Fiber to the home using a PON infrastructure. *J. Lightw. Technol.* **24**, 4568–4583 (2006)
- Majumdar, A.K.: Free-space laser communication performance in the atmospheric channel. *J. Opt. Fiber Commun. Rep.* **2**, 345–396 (2005)
- Manor, H., Arnon, S.: Performance of an optical wireless communication system as a function of wavelength. *Appl. Opt.* **42**(21), 4285–4294 (2003)
- Maru, K., Mizumoto, T., Uetsuka, H.: Demonstration of flat-passband multi/demultiplexer using multi-input arrayed waveguide grating combined with cascaded Mach-Zehnder interferometers. *J. Lightw. Technol.* **25**(8), 2187–2197 (2007)
- Mbah, A.M., Walker, J.G., Phillips, A.J.: Performance evaluation of digital pulse position modulation for wavelength division multiplexing FSO systems impaired by interchannel crosstalk. *IET Optoelectron.* **8**(6), 245–255 (2014)
- Mbah, A.M., Walker, J.G., Phillips, A.J.: Performance evaluation of turbulence-accentuated interchannel crosstalk for hybrid fibre and free space optical wavelength division multiplexing systems using digital pulse position modulation. *IET Optoelectron* **10**(1), 11–20 (2016)
- Mbah, A.M., Walker, J.G., Phillips, A.J.: Outage probability of WDM free-space optical systems affected by turbulence-accentuated interchannel crosstalk. *J. Phillips IET Optoelectron.* **11**(3), 91–97 (2017)
- Monroy, I.T., Tangdiongga, E.: *Crosstalk in WDM Communication Networks*. Kluwer Academic, Norwell, MA (2002)
- Ng, B., Ab-Rahman, M.S., Premadi, A., Jumari, K.: Optical power budget and cost analysis in PON-based *i*-FTTH. *Res. J. Inf. Technol.* **2**, 127–138 (2010)
- Phillips, A.J.: Power penalty for burst mode reception in the presence of interchannel crosstalk. *IET Optoelectron.* **1**, 127–134 (2007)
- Phillips, A.J., Cryan, R.A., Senior, J.M.: An optically preamplified intersatellite PPM receiver employing maximum likelihood detection. *IEEE Photon. Technol. Lett.* **8**(5), 691–693 (1996)
- Popoola, W.O., Ghassemlooy, Z.: BPSK Subcarrier intensity modulated free-space optical communications in Atmospheric turbulence. *J. Lightw. Technol.* **27**(8), 967–973 (2009)
- Ramaswami, R., Sivarajan, K.N.: *Optical Networks—A Practical Perspective*, 2nd edn. Academic, London (2002)
- Shapiro, J.H., Harney, R.C.: Burst-mode atmospheric optical communication. In: *Proceedings of National Telecommunication Conference*, pp. 27.5.1–27.5.7 (1980)
- Sibley, M.J.: *Optical Communications: Components and Systems*, 2nd edn. Macmillan Press Ltd, London (1995)
- Trinh, P.V., Dang, N.T., Thang, T.C., Pham, A.T.: Performance of all-optical amplify- and-forward WDM/FSO relaying systems over atmospheric dispersive turbulence channels. *IEICE Trans. Commun.* **99**(6), 1255–1264 (2016)
- Vetelino, F.S., Young, C., Andrews, L., Rekolons, J.: Aperture averaging effects on the probability density of irradiance fluctuations in moderate-to-strong turbulence. *Appl. Opt.* **46**(11), 2099–2108 (2007)
- Yang, L., Song, X., Cheng, J., Holzman, J.F.: Free-Space optical communications over lognormal fading channels using OOK with finite extinction ratios. *IEEE Access* **4**, 574–584 (2016)
- Yu, C.X., Neilson, D.T.: Diffraction-grating-based (de)multiplexer using image plane transformations. *IEEE J. Sel. Top. Quantum Electron.* **8**(6), 1194–1201 (2002)
- Zuo, T.J., Phillips, A.J.: Performance of burst mode receivers for optical digital pulse position modulation in passive optical network application. *IET Optoelectron.* **3**(3), 123–130 (2009)

## Affiliations

**Ebrahim Eld. Elsayed<sup>1</sup> · Bedir B. Yousif<sup>2</sup> · Mahmoud M. Alzalabani<sup>1</sup>**

Bedir B. Yousif  
bedir.yousif@gmail.com

Mahmoud M. Alzalabani  
mmalzalabani@yahoo.com

<sup>1</sup> Electronics and Communications Department, Faculty of Engineering, Mansoura University, Mansoura 35516, Egypt

<sup>2</sup> Electrical Engineering Department, Faculty of Engineering, Kafrelsheikh University, Kafrelsheikh 35514, Egypt